Bounds for the effective properties of heterogeneous plates

Trung-Kien Nguyen, Karam Sab, Guy Bonnet

Accepted Manuscript

Title: Bounds for the effective properties of heterogeneous plates

Authors: Trung-Kien Nguyen, Karam Sab, Guy Bonnet

PII: S0997-7538(09)00066-7

DOI: 10.1016/j.euromechsol.2009.05.006

Reference: EJMSOL 2530

To appear in: *European Journal of Mechanics / A Solids*

Received Date: 14 November 2008

Revised Date: 12 May 2009

Accepted Date: 23 May 2009

Please cite this article as: Nguyen, T.-K., Sab, K., Bonnet, G. Bounds for the effective properties of heterogeneous plates, European Journal of Mechanics / A Solids (2009), doi: 10.1016/j.euromechsol.2009.05.006

Bounds for the effective properties of heterogeneous plates

Trung-Kien NGUYEN[a], Karam SAB[a], Guy BONNET[*,b]

[a] *Université Paris-Est, UR Navier, Ecole des Ponts ParisTech, 6-8 Avenue Blaise Pascal, Champs-sur-Marne, 77455 Marne-La-Vallée Cedex 2, France*
[b] *Université Paris-Est, Laboratoire de Modélisation et Simulation Multi Echelle (FRE3160 CNRS), 5 bd Descartes, 77454 Marne-La-Vallée, France*

Abstract

This paper presents new bounds for heterogeneous plates which are similar to the well-known Hashin-Shtrikman bounds, but take into account plate boundary conditions. The Hashin-Shtrikman variational principle is used with a self-adjoint Greeen-operator with traction-free boundary conditions proposed by the authors. This variational formulation enables to derive lower and upper bounds for the effective in-plane and out-of-plane elastic properties of the plate. Two applications of the general theory are considered: first, in-plane invariant polarization fields are used to recover the "first-order" bounds proposed by Kolpakov(1999) for general heterogeneous plates; next, "second-order bounds" for n-phase plates whose constituents are statistically homogeneous in the in-plane directions are obtained. The results related to a two-phase material made of elastic isotropic materials are shown. The "second-order" bounds for the plate elastic properties are compared with the plate properties of homogeneous plates made of materials having an elasticity tensor computed from "second-order" Hashin-Shtrikman bounds in an infinite domain.

Key words: Hashin-Shtrikman variational principle, $\mathbf{\Gamma}$-operator, plate, Fourier transforms, second-order bounds, effective properties.

[*]Corresponding author
Email address: guy.bonnet@univ-paris-est.fr (Guy BONNET)

1 Introduction

The prediction of the effective properties of heterogeneous media from the material properties and from the geometrical arrangement of their constituting phases requires the solution of a boundary value problem on a representative volume. The characteristic size of this representative volume must be large enough compared to the one of the microstructure to ensure that the material can accurately be treated as homogeneous with spatially constant averages. If the geometrical arrangement of the heterogeneities within the medium is perfectly described, solving the boundary value problem is possible. Practically however, only a few features of the geometry (typically the volume fraction of each phase and low-order correlation functions) are known. In such a case, effective properties cannot be obtained exactly, but lower and upper bounds can be derived from variational principles.

The application of variational methods to composite materials was initiated by Hill (1952) who recovered the so-called Voigt and Reuss bounds. The classical variational principles usually require either compatible strain fields or self-balanced stress fields. The Hashin and Shtrikman (1962a,b) variational principles may be the most widely used since they lead to optimal bounds for the conductivity, bulk, and shear moduli of isotropic composites made of isotropic constituents. These principles are expressed in terms of polarization fields on which no constraint is imposed, contrarily to the case of classical variational formulations. Hashin and Shtrikman (1967) subsequently extended those principles to inhomogeneous elastic bodies subject to polarization fields and mixed boundary conditions. Willis (1977, 1981) summarized and generalized the Hashin-Shtrikman variational principles by using a $\mathbf{\Gamma}$-operator related to an infinite medium.

The homogenization of elastic periodic plates has been studied by many authors (Duvaut and Metellus, 1976; Caillerie, 1984; Kohn and Vogelius, 1984; Lewiński and Telega, 2000; Bourgeois et al., 1998; Cecchi and Sab, 2002a,b, 2004; Sab, 2003; Dallot and Sab, 2008a,b), but few of previous works were performed to obtain the bounds of plates properties.in Kolpakov (1999); Kolpakov and Sheremet (1999) and Kolpakov (1998) first order ("Voigt" and "Reuss") bounds were obtained for plates and the question arises naturally to find if more sophisticated bounds can be found , and more specifically if Hashin-Shtrikman bounds can be extended to plates. The answer to such a question is simple when the size of the heterogeneities is small compared to the thickness of the plate or when the thickness of the plate is small

compared to the (in-plane) size of the the heterogeneities. In the first case, bounds can be obtained for the plates containing isotropic composites made of isotropic constituents by computing Hashin and Shtrikman bounds for the filling material and by computing from it the stiffness properties of the plate. In the second case, the bounds can be computed from the Hashin and Shtrikman bounds computed from the plane stress properties of the components.

Obtaining the bounds in the case of heterogeneities whose size is comparable to the plate thickness is the subject of the present paper. A main feature of the Hashin-Shtrikman principle is that it uses the $\mathbf{\Gamma}$-operator of the homogeneous medium. If this principle must be extended to plates, a necessary ingredient is the $\mathbf{\Gamma}$-operator taking into account the stress-free boundary conditions of the plate. A new method for the computation of the effective elastic properties of a periodic plate was recently proposed by Nguyen et al. (2008). The theoretical derivations rely on a new $\mathbf{\Gamma}$-operator for periodic media with traction-free boundary conditions, on an iterative algorithm and on the use of the Fast Fourier Transform (FFT), in the line of methods used for homogenization of periodic media (Moulinec and Suquet, 1994, 1998; Bonnet, 2007). This new method was proved numerically efficient to estimate the effective elastic properties of plates. Based on this previous work (Nguyen et al., 2008), the present paper aims at using a Hashin-Shtrikman variational principle in the case of heterogeneous plates for supplying bounds of the effective in-plane and out-of-plane elastic stiffnesses by introducing into the variational principle the Γ-operator obtained by the authors.

Compared to the usual Hashin-Shtrikman bounds for infinite media , two main differences are taken into account here : the traction-free conditions on the surfaces of the plate and the inhomogeneous macroscopic strains and stresses for the case of bending. As explained before, the case of interest is when the thickness of the plate and the size of heterogeneities are of the same order. The thickness and the period of the plate are therefore assumed to be of the same order and small compared to the in-plane typical (macroscopic) size L of the plate. The stiffness constants of the plate can be bounded by introducing suitable polarization fields into the variational principle. Two applications of the theory are considered. In-plane invariant polarization fields are first used to recover the bounds proposed by Kolpakov (1999) for general heterogeneous plates. Secondly, n-phase plates whose constituents are distributed randomly but in a statistically uniform manner in the in-plane directions are studied. The derived energy functional expressed

in terms of the polarizations depends on the thickness-coordinate only and the computation of the effective elastic properties of the plate requires the use of a two-point distribution function. The example of a two-phase plate made of isotropic materials is considered. The derived bounds for the effective elastic properties of the plate are compared with the elastic properties of the plate computed from elasticity tensors obtained from the classical Hashin-Shtrikman bounds (Hashin and Shtrikman, 1962a,b, 1965) for an infinite two-phase medium. It must be emphasized that the computation of bounds presented thereafter do not use the computation of effective properties of a periodic medium, as effected in (Nguyen and al.(2008)). Similarly to the known HS bounds, the bounds are obtained directly from the variational principle and from assumptions related to the two-point probability function of heterogeneties distribution, without ensemble averaging or "cell computations". The Green tensor for the plate is used with wave lengths large enough compared to the size of heterogeneities.

The paper is organized as follows. In section 2, the Hashin-Shtrikman variational principle (Hashin and Shtrikman, 1962a,b; Willis, 1977, 1981; Drugan and Willis, 1996) is recalled and it is shown that it can be used by introducing the $\mathbf{\Gamma}$-operator for periodic media with traction-free boundary conditions (Nguyen et al., 2008), because this operator is self adjoint. Thus completed, this general variational formulation enables to derive lower and upper bounds for the effective elastic properties of heterogeneous plates. Section 3 presents an application of the results derived in section 2 by using polarization fields which are assumed to be invariant along the in-plane directions. In section 4, we apply the method to random materials whose constituents are distributed randomly but in a statistically uniform manner in the in-plane directions. The functional is expressed in terms of the in-plane invariant polarizations. Then a randomly distributed two-phase plate made of isotropic constituents is considered. An analysis of the effects of the size of heterogeneity is finally performed.

2 Theoretical Formulation

As it will be recalled thereafter from (Nguyen et al., 2008), the Green tensor for the plate can be computed for a periodic plate under the form of a series on the wave numbers associated to the dimensions of the rectangular chosen period. The result corresponds to a periodic repartition of singularities applied within an homogeneous plate. In order to obtain the bounds

for repartitions of heterogeneities which are not periodically distributed as in figure 1, the Green tensor must be obtained for an infinite domain. However, even if the Green tensor for the infinite homogeneous plate is obviously obtained when the sizes of the period tends to infinity, there is no closed form solution of the Fourier integral thus obtained. From another point of view, the Green tensor will be used associated via a convolution product with a correlation fonction whose support is practically finite. It is therefore possible to use the Green tensor associated to the periodic plate to perform such a convolution product with an error which can be as small as desired. From another point of view, heterogeneities within the plate will be assumed random within the plate. One more time, due to the finite support of the correlation function, the computation of bounds is not affected by using a random distribution of elastic properties within a period as soon as the correlation length is small compared to the period dimensions.

Finally, the problem which is considered here is the one related to a heterogeneous medium whithin a period, the heterogeneities being reproduced periodically. Such a solution will be used in section 4 for periods large compared to the correlation length.

The unit cell Y that generates the plate by periodicity in the (x_1, x_2)-directions is the 3D domain:

$$Y = \left\{ \mathbf{x} \in \mathbf{R}^3,\, \mathbf{x} = (x_1, x_2, x_3),\, x_i \in \left]-\frac{l_i}{2}, \frac{l_i}{2}\right[,\, i = 1,2,3 \right\}. \tag{1}$$

The domain $\omega = \left]-\frac{l_1}{2}, \frac{l_1}{2}\right[\times \left]-\frac{l_2}{2}, \frac{l_2}{2}\right[$ is the middle surface of the cell. $\partial\omega$ is the boundary of ω and $\partial Y_l = \partial\omega \times \left]-\frac{t}{2}, \frac{t}{2}\right[$ $(l_3 = t)$ is the lateral boundary of Y. The top and bottom surfaces of the cell are $\partial Y^{\pm} = \omega \times \{\pm\frac{t}{2}\}$. Mixed conditions are defined along the boundaries of the cell as follows: periodic boundary conditions are assumed along ∂Y_l while traction-free boundary conditions are assumed along $\partial Y^{\pm}$. All formulations are performed under the assumption of a linear elastic behavior and small deformations of materials. The Greek indices belong to $\{1, 2\}$ and the Latin indices to $\{1, 2, 3\}$.

The local elasticity problem defined on Y is:

$$\begin{cases} \boldsymbol{\sigma}(\mathbf{x})\,.\,\boldsymbol{\nabla} = 0,\ \boldsymbol{\sigma}(\mathbf{x}) = \mathbf{L}(\mathbf{x})\,\boldsymbol{\epsilon}(\mathbf{x}),\ \boldsymbol{\epsilon}(\mathbf{x}) = \mathbf{E} + x_3\boldsymbol{\chi} + \mathbf{e}(\mathbf{v}^{per}(\mathbf{x})), \\ \mathbf{e}(\mathbf{v}^{per}(\mathbf{x})) = \mathbf{v}^{per}(\mathbf{x}) \otimes^s \boldsymbol{\nabla}, \\ \boldsymbol{\sigma}(\mathbf{x})\,.\,\boldsymbol{e}_3 = 0 \quad \text{on}\, \partial Y^{\pm}, \\ \mathbf{v}^{per}(\mathbf{x}) \text{ periodic on}\, \partial Y_l, \quad \boldsymbol{\sigma}(\mathbf{x})\,.\,\mathbf{n} \text{ anti-periodic on}\, \partial Y_l, \end{cases} \tag{2}$$

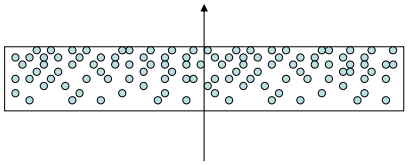

Figure 1: Example of plate containing a random distribution of heterogeneities.

where the nabla operator $\boldsymbol{\nabla}$ is used to express the gradient and divergence operators ($\mathbf{v}^{per} \otimes \boldsymbol{\nabla} = v^{per}_{i,j}\, \boldsymbol{e}_i \otimes \boldsymbol{e}_j$, $\boldsymbol{\sigma}\,.\,\boldsymbol{\nabla} = \sigma_{ij,j}\, \boldsymbol{e}_i$). $\boldsymbol{e}_i$ are the vectors of an orthogonal basis of the space, $\mathbf{v}^{per}(\mathbf{x})$ is the (x_1, x_2)-periodic displacement field, $\mathbf{e}(\mathbf{v}^{per}(\mathbf{x}))$ the corresponding strain field (the symmetrical part of $\mathbf{v}^{per}(\mathbf{x}) \otimes \boldsymbol{\nabla}$), $\boldsymbol{\epsilon}(\mathbf{x})$ the total strain field, $\mathbf{L}(\mathbf{x})$ the elasticity tensor and $\boldsymbol{\sigma}(\mathbf{x})$ the total stress field. The macroscopic membrane strains, $\mathbf{E}$, and the macroscopic curvatures, $\boldsymbol{\chi}$, only have in-plane components ($E_{j3} = 0, \chi_{j3} = 0$).

Once the solution of the boundary value problem (2) is obtained, the homogenized elastic properties of the plate are derived from the elastic strain energy expressed by:

$$W = \frac{1}{2} < \boldsymbol{\sigma}(\mathbf{x})\, \boldsymbol{\epsilon}(\mathbf{x}) >= \frac{1}{2} \left(\mathbf{N}\, \mathbf{E} + \mathbf{M}\, \boldsymbol{\chi} \right), \tag{3}$$

where the brackets $< \,.\, >$ correspond to the following average operator

on the unit cell:

$$< f >= \frac{1}{|\omega|} \int_Y f(\mathbf{x})\, d\mathbf{x}. \tag{4}$$

$\mathbf{N}$ is the membrane stress tensor and $\mathbf{M}$ is the flexure moment tensor:

$$N_{\alpha\beta} =< \sigma_{\alpha\beta} >, \quad M_{\alpha\beta} =< x_3\, \sigma_{\alpha\beta} > . \tag{5}$$

Equation (3) can be interpreted as the macro-homogeneity condition of Hill-Mandel which ensures that the macroscopic elastic strain energy of a given representative volume element is equal to the integral of the microscopic elastic strain energy within this volume.

Hence, the strain energy per unit area becomes:

$$W = \frac{1}{2} < \boldsymbol{\sigma}(\mathbf{x})\, \boldsymbol{\epsilon}(\mathbf{x}) >= \frac{1}{2} \left(\mathbf{E}\mathbf{A}\mathbf{E} + 2\mathbf{E}\mathbf{B}\boldsymbol{\chi} + \boldsymbol{\chi}\mathbf{D}\boldsymbol{\chi} \right), \tag{6}$$

where the homogenized elastic tensors $(\mathbf{A}, \mathbf{B}, \mathbf{D})$ of the plate are:

$$\mathbf{N} = \mathbf{A}\,\mathbf{E} + \mathbf{B}\,\boldsymbol{\chi}, \quad \text{and} \quad \mathbf{M} = \mathbf{B}^T\,\mathbf{E} + \mathbf{D}\,\boldsymbol{\chi}, \tag{7}$$

where the superscript T is the transposition operator.

The elasticity problem (2) may be solved along the lines of Suquet (1990) by introducing a homogeneous reference medium of stiffness $\mathbf{L}^o$ and a polarization field, $\boldsymbol{\tau}$:

$$\begin{cases} \boldsymbol{\sigma}(\mathbf{x})\,.\,\boldsymbol{\nabla} = 0,\ \boldsymbol{\sigma}(\mathbf{x}) = \mathbf{L}^o\,\boldsymbol{\epsilon}(\mathbf{x}) + \boldsymbol{\tau}(\mathbf{x}),\ \boldsymbol{\epsilon}(\mathbf{x}) = \mathbf{E} + x_3\boldsymbol{\chi} + \mathbf{e}(\mathbf{v}^{per}(\mathbf{x})), \\ \mathbf{e}(\mathbf{v}^{per}(\mathbf{x})) = \mathbf{v}^{per}(\mathbf{x}) \otimes^s \boldsymbol{\nabla}, \\ \boldsymbol{\sigma}(\mathbf{x})\,.\,\boldsymbol{e}_3 = 0 \quad \text{on}\, \partial Y^{\pm}, \\ \mathbf{v}^{per}(\mathbf{x}) \text{ periodic on}\, \partial Y_l, \quad \boldsymbol{\sigma}(\mathbf{x})\,.\,\mathbf{n} \text{ anti-periodic on}\, \partial Y_l, \end{cases} \tag{8}$$

where the polarization field $\boldsymbol{\tau}(\mathbf{x})$ is given by:

$$\boldsymbol{\tau}(\mathbf{x}) = \delta\mathbf{L}(\mathbf{x})\,\boldsymbol{\epsilon}(\mathbf{x}) \quad \text{with} \quad \delta\mathbf{L}(\mathbf{x}) = \mathbf{L}(\mathbf{x}) - \mathbf{L}^o. \tag{9}$$

We note that the elasticity problem (8) with $(\mathbf{E}, \boldsymbol{\chi}, \boldsymbol{\tau})$ can be split into two auxiliary problems:

- An auxiliary problem which is identical to the elasticity problem (8) but in which $\boldsymbol{\tau} = 0$. It coincides with the set of equations (2) for $\mathbf{L}(\mathbf{x}) = \mathbf{L}^o$ and admits the fields $(\boldsymbol{\sigma}^o, \boldsymbol{\epsilon}^o, \mathbf{v}_o^{per})$ as a solution.

- Another auxiliary problem identical to the elasticity problem (8) but in which $\mathbf{E} = 0$ and $\boldsymbol{\chi} = 0$. This second auxiliary problem admits the fields $(\boldsymbol{\sigma}^{per}, \mathbf{e}(\mathbf{u}^{per}), \mathbf{u}^{per})$ as a solution.

As a result, the fields solution of the elasticity problem (8) with $(\mathbf{E}, \boldsymbol{\chi}, \boldsymbol{\tau})$ are the superposition of $(\boldsymbol{\sigma}^o, \boldsymbol{\epsilon}^o, \mathbf{v}_o^{per})$ with $(\boldsymbol{\sigma}^{per}, \mathbf{e}(\mathbf{u}^{per}), \mathbf{u}^{per})$.

2.1 Homogeneous Solutions in the Reference Medium

This section is devoted to the first auxiliary problem introduced in the previous section. The fields $(\boldsymbol{\sigma}^o(\mathbf{x}), \boldsymbol{\epsilon}^o(\mathbf{x}), \mathbf{v}_o^{per}(\mathbf{x}))$ which are solutions of the local elasticity problem (2) defined on the reference medium with stiffness $\mathbf{L}^o$ are derived from the following system of equations:

$$\left\{\begin{array}{l} \boldsymbol{\sigma}^o(\mathbf{x}) \,.\, \boldsymbol{\nabla} = 0,\ \boldsymbol{\sigma}^o(\mathbf{x}) = \mathbf{L}^o\, \boldsymbol{\epsilon}^o(\mathbf{x}),\ \boldsymbol{\epsilon}^o(\mathbf{x}) = \mathbf{E} + x_3\boldsymbol{\chi} + \mathbf{e}^o(\mathbf{v}_o^{per}(\mathbf{x})), \\ \mathbf{e}^o(\mathbf{v}_o^{per}(\mathbf{x})) = \mathbf{v}_o^{per}(\mathbf{x}) \otimes^s \boldsymbol{\nabla}, \\ \boldsymbol{\sigma}^o(\mathbf{x}) \,.\, \boldsymbol{e}_3 = 0 \quad \text{on} \quad \partial Y^{\pm}, \\ \mathbf{v}_o^{per}(\mathbf{x}) \text{ periodic on } \partial Y_l, \quad \boldsymbol{\sigma}^o(\mathbf{x}) \,.\, \mathbf{n} \text{ anti-periodic on } \partial Y_l, \end{array}\right. \tag{10}$$

This problem has a trivial solution, $(\boldsymbol{\sigma}^o(x_3), \boldsymbol{\epsilon}^o(x_3), \mathbf{v}_o^{per}(x_3))$, that depends on x_3 only. This trivial solution can be derived directly by solving the ordinary differential equations in x_3 for given boundary conditions. To this aim, the stresses and strains are split into their in-plane and out-of-plane components:

$$\left\{\begin{array}{ll} \boldsymbol{\sigma}^o_{(i)} = (\sigma^o_{11}, \sigma^o_{22}, \sigma^o_{12})^T, & \boldsymbol{\sigma}^o_{(o)} = (\sigma^o_{33}, \sigma^o_{23}, \sigma^o_{13})^T, \\ \boldsymbol{\epsilon}^o_{(i)} = (\epsilon^o_{11}, \epsilon^o_{22}, 2\epsilon^o_{12})^T, & \boldsymbol{\epsilon}^o_{(o)} = (\epsilon^o_{33}, 2\epsilon^o_{23}, 2\epsilon^o_{13})^T, \end{array}\right. \tag{11}$$

where the indices (i) and (o) indicate the in-plane and out-of-plane components, respectively. Similarly, the reference elasticity tensor $\mathbf{L}^o$ is also split into four 3×3 matrices: The in-plane components $\mathbf{L}^o_{(i)(i)}$, the coupling components $\mathbf{L}^o_{(i)(o)}$ and $\mathbf{L}^o_{(o)(i)}$, and the out-of-plane components $\mathbf{L}^o_{(o)(o)}$. $\mathbf{L}^o_{(i)(i)}$ and $\mathbf{L}^o_{(o)(o)}$ are symmetrical while $\mathbf{L}^o_{(i)(o)}$ and $\mathbf{L}^o_{(o)(i)}$ verify $(\mathbf{L}^o_{(i)(o)})^T = \mathbf{L}^o_{(o)(i)}$.

The constitutive equations thus become:

$$\left\{\begin{array}{l} \boldsymbol{\sigma}^o_{(i)}(x_3) = \mathbf{L}^o_{(i)(i)}\boldsymbol{\epsilon}^o_{(i)}(x_3) + \mathbf{L}^o_{(i)(o)}\boldsymbol{\epsilon}^o_{(o)}(x_3), \\ \boldsymbol{\sigma}^o_{(o)}(x_3) = \mathbf{L}^o_{(o)(i)}\boldsymbol{\epsilon}^o_{(i)}(x_3) + \mathbf{L}^o_{(o)(o)}\boldsymbol{\epsilon}^o_{(o)}(x_3). \end{array}\right. \tag{12}$$

One observes that the in-plane strains are equal to the macroscopic strains, i.e., $\boldsymbol{\epsilon}^o_{(i)}(x_3) = \mathbf{E}_{(i)} + x_3\boldsymbol{\chi}_{(i)}$, since the in-plane components of $\mathbf{e}^o(\mathbf{v}_o^{per})$ are

zero. Moreover, from the balance equations and the boundary conditions, one finds out that the out-of-plane stresses $\boldsymbol{\sigma}^o_{(o)}(x_3)$ are also zero. Hence, the out-of-plane strains can be expressed in terms of the in-plane strains:

$$\boldsymbol{\epsilon}^o_{(o)}(x_3) = -(\mathbf{L}^o_{(o)(o)})^{-1}\,\mathbf{L}^o_{(o)(i)}\,\boldsymbol{\epsilon}^o_{(i)}(x_3). \tag{13}$$

Substituting (13) into the first equation of (12), one links the in-plane stresses to the in-plane strains:

$$\boldsymbol{\sigma}^o_{(i)}(x_3) = \mathbf{L}^o_{(s)}\,\boldsymbol{\epsilon}^o_{(i)}(x_3), \tag{14}$$

where

$$\mathbf{L}^o_{(s)} = \mathbf{L}^o_{(i)(i)} - \mathbf{L}^o_{(i)(o)}\,(\mathbf{L}^o_{(o)(o)})^{-1}\,\mathbf{L}^o_{(o)(i)} = (\mathbf{L}^{o-1}_{(i)(i)})^{-1} \tag{15}$$

is the plane-stress elastic stiffness matrix of the reference medium.

2.2 Self-adjoint property of the $\boldsymbol{\Gamma}$*-Operator for the plate*

This section is devoted to the second auxiliary problem introduced in section 2 which is solved by the $\boldsymbol{\Gamma}$-Operator for the plate. This second auxiliary problem corresponds to Eqs. (8) in which $\mathbf{E} = 0$ and $\boldsymbol{\chi} = 0$:

$$\left\{\begin{array}{l} \boldsymbol{\sigma}^{per}(\mathbf{x})\,.\,\boldsymbol{\nabla} = 0,\ \boldsymbol{\sigma}^{per}(\mathbf{x}) = \mathbf{L}^o\,\mathbf{e}(\mathbf{u}^{per}(\mathbf{x})) + \boldsymbol{\tau}(\mathbf{x}), \\ \mathbf{e}(\mathbf{u}^{per}(\mathbf{x})) = \mathbf{u}^{per}(\mathbf{x}) \otimes^s \boldsymbol{\nabla}, \\ \boldsymbol{\sigma}^{per}(\mathbf{x})\,.\,\boldsymbol{e}_3 = 0 \quad \text{on} \quad \partial Y^{\pm}, \\ \mathbf{u}^{per}(\mathbf{x}) \text{ periodic on } \partial Y_l, \quad \boldsymbol{\sigma}^{per}(\mathbf{x})\,.\,\mathbf{n} \text{ anti-periodic on } \partial Y_l, \end{array}\right. \tag{16}$$

where the polarization tensor is given by Eq. (9). Eqs. (16) is solved by using a $\boldsymbol{\Gamma}$-operator which produces the total strain $\mathbf{e}(\mathbf{x})$ in terms of $\boldsymbol{\tau}$:

$$\mathbf{e} = -\boldsymbol{\Gamma}\boldsymbol{\tau} \tag{17}$$

The expression of the $\boldsymbol{\Gamma}$-operator was obtained by Nguyen et al. (2008). Following the procedure used in this paper, the field $\mathbf{u}^{per}(\mathbf{x})$ solution of Eqs. (16) is split into two terms: $\mathbf{u}^{per}(\mathbf{x}) = \mathbf{u}^p(\mathbf{x}) + \mathbf{u}^h(\mathbf{x})$. $\mathbf{u}^p(\mathbf{x})$ is obtained with the standard periodicity conditions in the x_3-direction and the complementary term $\mathbf{u}^h(\mathbf{x})$ enables to recover the stress-free boundary conditions. Likewise, the total strain and the $\boldsymbol{\Gamma}$-operator are expressed as $\mathbf{e} = \mathbf{e}^p + \mathbf{e}^h$ and $\boldsymbol{\Gamma} = \boldsymbol{\Gamma}_p + \boldsymbol{\Gamma}_h$ where $\mathbf{e}^p$ and $\boldsymbol{\Gamma}_p$ correspond to the standard periodic problem and $\mathbf{e}^h$ and $\boldsymbol{\Gamma}_h$ to the complementary problem.

The boundary value problem (16) can be solved by expanding the polarization field $\boldsymbol{\tau}(\mathbf{x}) \in \mathbf{L}^2(Y)$ into three-dimensional Fourier series (see Eq. (71)). The periodic strain field $\mathbf{e}^p(\mathbf{x})$ solution of Eqs. (16) is derived from:

$$\left\{ \begin{array}{l} \boldsymbol{\sigma}^p(\mathbf{x}) \,.\, \boldsymbol{\nabla} = 0,\, \boldsymbol{\sigma}^p(\mathbf{x}) = \mathbf{L}^o\, \mathbf{e}^p(\mathbf{x}) + \boldsymbol{\tau}(\mathbf{x}),\, \mathbf{e}^p(\mathbf{x}) = \mathbf{u}^p(\mathbf{x}) \otimes^s \boldsymbol{\nabla}, \\ \mathbf{u}^p(\mathbf{x}) \text{ periodic on } \partial Y, \quad \boldsymbol{\sigma}^p(\mathbf{x}) \,.\, \mathbf{n} \text{ anti-periodic on } \partial Y. \end{array} \right. \tag{18}$$

$\mathbf{e}^p(\mathbf{x})$ can be explicitly derived in the Fourier space (see Suquet (1990); Moulinec and Suquet (1994) for details). It is then used to define the corresponding self-adjoint periodic $\boldsymbol{\Gamma}_p$-operator defined by (see appendix A for details):

$$\mathbf{e}^p(\mathbf{x}) = -\frac{1}{|Y|} \int_Y \boldsymbol{\Gamma}_p(\mathbf{x} - \mathbf{x}')\, \boldsymbol{\tau}(\mathbf{x}')\, d\mathbf{x}'. \tag{19}$$

In contrast, the strain field $\mathbf{e}^h(\mathbf{x})$ and the related operator $\boldsymbol{\Gamma}_h(\mathbf{x})$ are derived by solving:

$$\left\{ \begin{array}{l} \boldsymbol{\sigma}^h(\mathbf{x}) \,.\, \boldsymbol{\nabla} = 0,\, \boldsymbol{\sigma}^h(\mathbf{x}) = \mathbf{L}^o\, \mathbf{e}^h(\mathbf{x}),\, \mathbf{e}^h(\mathbf{x}) = \mathbf{u}^h(\mathbf{x}) \otimes^s \boldsymbol{\nabla}, \\ \sigma^h_{j3}(\mathbf{x}) = -\sigma^p_{j3}(\mathbf{x}) \quad \text{on} \quad \partial Y^{\pm}, \\ \mathbf{u}^h(\mathbf{x}) \text{ periodic on } \partial Y_l, \quad \boldsymbol{\sigma}^h(\mathbf{x}) \,.\, \mathbf{n} \text{ anti-periodic on } \partial Y_l. \end{array} \right. \tag{20}$$

Eqs. (20) were solved by Nguyen et al. (2008) by using Fourier transforms along (x_1, x_2)-directions. $\mathbf{e}^h$ and the corresponding operator $\boldsymbol{\Gamma}_h$ are linked by:

$$\mathbf{e}^h(\mathbf{x}) = -\frac{1}{|Y|} \int_Y \boldsymbol{\Gamma}_h(\tilde{\mathbf{x}} - \tilde{\mathbf{x}}', x_3, x_3')\, \boldsymbol{\tau}(\mathbf{x}')\, d\mathbf{x}', \tag{21}$$

where the $\boldsymbol{\Gamma}_h$-operator is periodic in the (x_1, x_2)-directions and $(\tilde{\mathbf{x}} - \tilde{\mathbf{x}'}, x_3, x_3')$ holds for $(x_1 - x_1', x_2 - x_2', x_3, x_3')$ (see appendix A for details).

Since $\boldsymbol{\Gamma} = \boldsymbol{\Gamma}_p + \boldsymbol{\Gamma}_h$ and since $\boldsymbol{\Gamma}$ is a self-adjoint operator, $\boldsymbol{\Gamma}_h$ is also a self-adjoint operator. The self-adjoint character of $\boldsymbol{\Gamma}$ can be directly inferred from Eqs. (16). To this aim, let us consider a kinematically admissible field, $\mathbf{e}(\mathbf{x}) \in \mathscr{U}$, and a statically admissible stress field, $\boldsymbol{\sigma}(\mathbf{x}) \in \mathscr{S}$, where:

$$\mathscr{U} = \Big\{ \mathbf{e}(\mathbf{x}) \Big/ \mathbf{e}(\mathbf{x}) = \mathbf{u}^{per}(\mathbf{x}) \otimes^s \boldsymbol{\nabla},\, \mathbf{u}^{per}(\mathbf{x}) \text{ periodic on } \partial Y_l \Big\}, \tag{22}$$

$$\mathscr{S} = \Big\{ \boldsymbol{\sigma}(\mathbf{x}) \Big/ \boldsymbol{\sigma} \,.\, \boldsymbol{\nabla} = 0,\, \boldsymbol{\sigma} \,.\, \boldsymbol{e}_3 = 0 \text{ on } \partial Y^{\pm}, \boldsymbol{\sigma} \,.\, \mathbf{n} \text{ antiperiodic on } \partial Y_l \Big\} \tag{23}$$

For all fields $(\boldsymbol{\sigma}_1, \mathbf{e}_1)$ and $(\boldsymbol{\sigma}_2, \mathbf{e}_2)$ solutions of Eqs. (16) with polarization fields $\boldsymbol{\tau}_1$ or $\boldsymbol{\tau}_2$, respectively, $\boldsymbol{\sigma}_1$ and $\boldsymbol{\sigma}_2$ are statically admissible and $\mathbf{e}_1$ and $\mathbf{e}_2$ are kinematically admissible. From Green's theorem, they verify:

$$< \boldsymbol{\sigma}_1 \, \mathbf{e}_2 >_Y = 0, \quad \text{and} \quad < \boldsymbol{\sigma}_2 \, \mathbf{e}_1 >_Y = 0. \tag{24}$$

Substituting the stress field, $\boldsymbol{\sigma} = \mathbf{L}^o \mathbf{e} + \boldsymbol{\tau}$, into Eq. (24) yields:

$$< \boldsymbol{\tau}_1 \, \mathbf{e}_2 >_Y = - < \mathbf{e}_1 \mathbf{L}^o \mathbf{e}_2 >_Y, \quad < \boldsymbol{\tau}_2 \, \mathbf{e}_1 >_Y = - < \mathbf{e}_2 \mathbf{L}^o \mathbf{e}_1 >_Y . \tag{25}$$

From the symmetry of the elasticity tensor $\mathbf{L}^o$, we have $< \boldsymbol{\tau}_1 \, \mathbf{e}_2 >_Y = < \boldsymbol{\tau}_2 \, \mathbf{e}_1 >_Y$. The $\boldsymbol{\Gamma}$-operator links strains to polarization fields:

$$\mathbf{e}_1 = -\boldsymbol{\Gamma} \boldsymbol{\tau}_1 \quad \text{and} \quad \mathbf{e}_2 = -\boldsymbol{\Gamma} \boldsymbol{\tau}_2. \tag{26}$$

Therefore,

$$< \boldsymbol{\tau}_1 \, \boldsymbol{\Gamma} \boldsymbol{\tau}_2 >_Y = < \boldsymbol{\tau}_2 \, \boldsymbol{\Gamma} \boldsymbol{\tau}_1 >_Y = < \mathbf{e}_1 \mathbf{L}^o \mathbf{e}_2 >_Y \quad \forall \boldsymbol{\tau}_1, \boldsymbol{\tau}_2, \tag{27}$$

which proves that $\boldsymbol{\Gamma}$ is a self-adjoint operator. Setting $\boldsymbol{\tau}_1 = \boldsymbol{\tau}_2$ in Eq. (27) also shows that $\boldsymbol{\Gamma}$ is positive. Combining Eq. (27) with Eq. (26) yields: $\boldsymbol{\Gamma} = \boldsymbol{\Gamma} \, \mathbf{L}^o \, \boldsymbol{\Gamma}$. Finally, since $\boldsymbol{\Gamma}_p$ is a self-adjoint operator, $\boldsymbol{\Gamma}_h$ also is a self-adjoint operator and verifies:

$$< \boldsymbol{\tau}_1 \, \mathbf{e}_2^h >_Y = < \boldsymbol{\tau}_2 \, \mathbf{e}_1^h >_Y \quad \text{or} \quad < \boldsymbol{\tau}_1 \, \boldsymbol{\Gamma}_h \boldsymbol{\tau}_2 >_Y = < \boldsymbol{\tau}_2 \, \boldsymbol{\Gamma}_h \boldsymbol{\tau}_1 >_Y . \tag{28}$$

2.3 Hashin-Shtrikman functional and variational principle

As shown in the previous subsection, the Green operator for the plate is self adjoint. It is therefore possible to introduce this Green operator into the Hashin-Shtrikman variational principle (Hashin and Shtrikman, 1962a,b, 1967; Willis, 1977, 1981).

The effective properties are obtained from the mean elastic energy denoted by W_{eff} :

$$W_{eff} = \frac{1}{2} < \boldsymbol{\sigma} \, \boldsymbol{\epsilon} > = \frac{1}{2} < \boldsymbol{\sigma} \, \boldsymbol{\epsilon}^o > . \tag{29}$$

The Hashin-Shtrikman principle can be written by using the functional $W(\boldsymbol{\tau})$ defined by :

$$W(\boldsymbol{\tau}) = \frac{1}{2} < \boldsymbol{\epsilon}^o \mathbf{L}^o \boldsymbol{\epsilon}^o > + \frac{1}{2} < 2 \boldsymbol{\tau} \boldsymbol{\epsilon}^o - \boldsymbol{\tau} \, \delta \mathbf{L}^{-1} \, \boldsymbol{\tau} - \boldsymbol{\tau} \, \boldsymbol{\Gamma} \boldsymbol{\tau} > . \tag{30}$$

When τ is the polarization field solution of the equilibrium equation, the value of the functional is equal to the mean energy W_{eff}. This functional can be split into two parts $W(\boldsymbol{\tau}) = W_o + W_1(\boldsymbol{\tau})$, where:

$$W_o = \frac{1}{2} < \boldsymbol{\epsilon}^o \, \mathbf{L}^o \, \boldsymbol{\epsilon}^o >= \frac{1}{2} \int_{-t/2}^{t/2} \boldsymbol{\epsilon}^o_{(i)}(x_3) \, \mathbf{L}^o_{(s)} \, \boldsymbol{\epsilon}^o_{(i)}(x_3) \, dx_3, \tag{31}$$

and:

$$W_1(\boldsymbol{\tau}) = \frac{1}{2} < 2\boldsymbol{\tau} \, \boldsymbol{\epsilon}^o - \boldsymbol{\tau} \, \delta\mathbf{L}^{-1} \, \boldsymbol{\tau} - \boldsymbol{\tau} \, \boldsymbol{\Gamma} \, \boldsymbol{\tau} > . \tag{32}$$

Eq. (31) shows that W_o can be explicitly calculated and does not depend on $\boldsymbol{\tau}$.

The variational principle associated to the functional may be expressed as :

$$\begin{cases} W_{eff} = Max_{\boldsymbol{\tau}}(W_o + W_1(\boldsymbol{\tau})) & \delta\mathbf{L} > 0, \\ W_{eff} = Min_{\boldsymbol{\tau}}(W_o + W_1(\boldsymbol{\tau})) & \delta\mathbf{L} < 0, \end{cases} \tag{33}$$

Hence Eqs. (33) can supply lower and upper bounds for the effective elastic properties of the plate. The functional $W_1(\boldsymbol{\tau})$ will be considered in more details in the following sections. Eqs. (33) show also that the lower and upper bounds depend on the properties of the reference medium. An optimization on the reference medium will thus yield optimal bounds.

3 First order Bound Estimates for (x_1, x_2)-Invariant Polarization Fields

Different bounds can be obtained for the properties of plates, depending of the assumptions on the distribution of the heterogeneities. In this section we introduce (x_1, x_2)-invariant polarization fields (i.e., $\boldsymbol{\tau}(\mathbf{x}) = \boldsymbol{\tau}(x_3)$) in the variational formulation. As it will be shown thereafter, the solution will be closely related to the properties of stratified plates. Therefore, a laminated plate with elastic properties that are (x_1, x_2)-independent (i.e., $\mathbf{L}(\mathbf{x}) = \mathbf{L}(x_3)$) as in figure 2 is first considered. In such a case, the fields solution of Eqs. (2) are invariant in the (x_1, x_2)-directions: $(\boldsymbol{\sigma}(\mathbf{x}), \boldsymbol{\epsilon}(\mathbf{x}), \mathbf{v}(\mathbf{x})) = (\boldsymbol{\sigma}(x_3), \boldsymbol{\epsilon}(x_3), \mathbf{v}(x_3))$. Hence, as is the case with homogeneous plates, the solution can be obtained analytically and the overall elastic properties of the plate are given by:

$$(\mathbf{A}, \mathbf{B}, \mathbf{D}) = \int_{-t/2}^{t/2} (1, x_3, x_3^2) \, \mathbf{L}_{(s)}(x_3) \, dx_3, \tag{34}$$

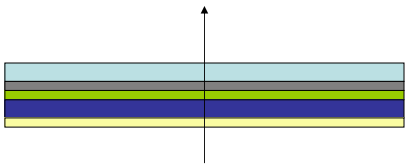

Figure 2: Example of a stratified distribution of polarization tensor (homogeneous in each layer) which is used to compute the bounds.

where it is recalled that the matrices $\mathbf{A}, \mathbf{B}, \mathbf{D}$ were defined in (7) and where $\mathbf{L}_{(s)}(x_3)$ is the plane-stress elasticity matrix at x_3 which verifies Eq. (15).

Moreover, for any $\mathbf{L}'(x_3) \geq \mathbf{L}(x_3)$ we have:

$$(\mathbf{A}', \mathbf{B}', \mathbf{D}') \geq (\mathbf{A}, \mathbf{B}, \mathbf{D}), \tag{35}$$

in the sense of the corresponding strain energy.

Let us consider the more general case $\mathbf{L}(\mathbf{x}) = \mathbf{L}(x_1, x_2, x_3)$. In such a case the functional W_1 in (32) is given by:

$$W_1(\boldsymbol{\tau}) = \frac{1}{2} \int_{-t/2}^{t/2} \left[2\boldsymbol{\tau}(x_3)\boldsymbol{\epsilon}^o(x_3) - \boldsymbol{\tau}(x_3)\, \overline{\delta \mathbf{L}^{-1}}(x_3)\boldsymbol{\tau}(x_3) - \boldsymbol{\tau}(x_3)\boldsymbol{\Gamma}\boldsymbol{\tau}(x_3) \right] dx_3, \tag{36}$$

where $\overline{\mathbf{f}}(x_3)$ is the (x_1, x_2)-average of $\mathbf{f}(x_1, x_2, x_3)$:

$$\overline{\mathbf{f}}(x_3) = \frac{1}{|\omega|} \int \mathbf{f}(x_1, x_2, x_3)\, dx_1 dx_2. \tag{37}$$

In the present case, the functional can be computed as for a material which is layered in the thickness of the plate because the integrand in $W_1(\boldsymbol{\tau})$ depends on x_3 only. Let us therefore introduce the tensor $\mathbf{L}^*(x_3)$, related to a stratified plate, which is given by :

$$\mathbf{L}^*(x_3) = \left(\overline{\delta \mathbf{L}^{-1}}(x_3)\right)^{-1} + \mathbf{L}^o, \tag{38}$$

The homogenized stiffnesses of the plate related to this tensor are given by : $(\mathbf{A}^*, \mathbf{B}^*, \mathbf{D}^*)$:

$$(\mathbf{A}^*, \mathbf{B}^*, \mathbf{D}^*) = \int_{-t/2}^{t/2} (1, x_3, x_3^2)\, \mathbf{L}^*_{(s)}(x_3)\, dx_3. \tag{39}$$

Equation (33) yields:

$$\begin{cases} (\mathbf{A}, \mathbf{B}, \mathbf{D}) \geq (\mathbf{A}^*, \mathbf{B}^*, \mathbf{D}^*) & \forall \mathbf{L}^o,\ \delta \mathbf{L} > 0, \\ (\mathbf{A}, \mathbf{B}, \mathbf{D}) \leq (\mathbf{A}^*, \mathbf{B}^*, \mathbf{D}^*) & \forall \mathbf{L}^o,\ \delta \mathbf{L} < 0. \end{cases} \tag{40}$$

The bounds for the homogenized elastic properties of the plate vary with the reference medium and can therefore be optimized by an appropriate choice of the reference medium. To this aim, one considers the following two limit problems: $\mathbf{L}^o$ tends to zero and $\mathbf{L}^o$ tends to infinity.

For the case $\mathbf{L}^o \to \infty$ and $\delta \mathbf{L} < 0$, with no loss of generality, one can write $\mathbf{L}^o = \beta \mathbf{I}$ where $\mathbf{I}$ is the unit matrix and β is a positive coefficient which tends to infinity. One performs the following transformations:

$$\overline{\delta \mathbf{L}^{-1}}(x_3) = \overline{[\mathbf{L}(\mathbf{x}) - \mathbf{L}^o]^{-1}} = -\beta^{-1} \overline{[\mathbf{I} - \beta^{-1} \mathbf{L}(\mathbf{x})]^{-1}}. \tag{41}$$

By using the expansion:

$$(\mathbf{I} - \mathbf{X})^{-1} = \mathbf{I} + \mathbf{X} + \mathbf{X}^2 + \ldots \quad \forall \mathbf{X}, ||\mathbf{X}|| < \mathbf{1}, \tag{42}$$

equation (41) becomes:

$$\overline{\delta \mathbf{L}^{-1}}(x_3) = -\beta^{-1} [\mathbf{I} + \beta^{-1} \overline{\mathbf{L}}(x_3) + \beta^{-2} \overline{\mathbf{L}^2}(x_3) + \ldots]. \tag{43}$$

The high-order terms in Eq. (43) can be neglected when $\beta \to \infty$. Hence, by making use of Eq. (42) again for $\left(\overline{\delta \mathbf{L}^{-1}}(x_3)\right)^{-1}$, one obtains:

$$\mathbf{L}^*(x_3) \to \overline{\mathbf{L}}(x_3) \quad \text{when} \quad \beta \to \infty. \tag{44}$$

We prove next that the limit value obtained above, $\overline{\mathbf{L}}(x_3)$, is the best bound. It means that this is the minimum value of $\mathbf{L}^*(x_3)$, i.e., $\mathbf{L}^*(x_3) \geq \overline{\mathbf{L}}(x_3)$ with $\delta\mathbf{L} < 0$. This proof requires the following inequality to be verified:

$$\left(\overline{\delta \mathbf{L}^{-1}}(x_3)\right)^{-1} \geq \overline{\mathbf{L}}(x_3) - \mathbf{L}^o = \overline{\delta \mathbf{L}}(x_3). \tag{45}$$

By substituting $\mathbf{M} = -\delta\mathbf{L} > 0$ into Eq. (45), one recovers the inequality between the Voigt and Reuss bounds: $\overline{\mathbf{M}} \geq \left(\overline{\mathbf{M}^{-1}}\right)^{-1}$. Therefore Eq. (45) is satisfied for any $\delta\mathbf{L} < 0$ and the limit value $\overline{\mathbf{L}}(x_3)$ yields the optimal upper bound for the effective in-plane and out-of-plane elastic properties of the plate:

$$(\mathbf{A}^*, \mathbf{B}^*, \mathbf{D}^*)^+ = \int_{-t/2}^{t/2} (1, x_3, x_3^2)\, \overline{\mathbf{L}}_{(s)}(x_3)\, dx_3 \tag{46}$$

or

$$(\mathbf{A}^*, \mathbf{B}^*, \mathbf{D}^*)^+ = \int_{-t/2}^{t/2} (1, x_3, x_3^2)\, (\overline{\mathbf{L}}^{-1}_{(i)(i)})^{-1}(x_3)\, dx_3. \tag{47}$$

It means that this bound is computed as follows : in a first step, the mean value of the elasticity tensor for each plane parallel to the mean plane of the plate is computed. This allows to define a stratified plate whose properties are these mean properties. The stiffnesses of the plates are bounded by the stiffness of a homogeneous plate whose properties are obtained by the Voigt bound. It is worthwile to notice that the value of $\mathbf{L_0}$ leading to the bound is not the elasticity tensor used for the classical derivation of Hashin-Shtrikman bounds, which is finite (as in the next subsection).

The other bound can be obtained as follows : for the case $\mathbf{L}^o \to 0$ and $\delta\mathbf{L} > 0$, from Eq. (38) follows $\mathbf{L}^*(x_3) \to \left(\overline{\mathbf{L}^{-1}}\right)^{-1}$. We prove next that $\left(\overline{\mathbf{L}^{-1}}\right)^{-1}$ is the maximum value of $\mathbf{L}^*(x_3)$. To this aim, the inequality $\mathbf{L}^*(x_3) \leq \left(\overline{\mathbf{L}^{-1}}\right)^{-1}$ with $\delta\mathbf{L} > 0$ has to be verified.

Since for any $\mathbf{G} \geq 0$, $\left(\overline{\mathbf{G}^{-1}}\right)^{-1}$ is concave, the following relation holds for any $\mathbf{G}_1 \geq 0$ and $\mathbf{G}_2 \geq 0$ and $\lambda \in [0,1]$:

$$\left(\overline{(\lambda\mathbf{G}_1 + (1-\lambda)\mathbf{G}_2)^{-1}}\right)^{-1} \geq \lambda \left(\overline{\mathbf{G}_1^{-1}}\right)^{-1} + (1-\lambda)\left(\overline{\mathbf{G}_2^{-1}}\right)^{-1}. \tag{48}$$

Substituting $\mathbf{G}_1 = \delta\mathbf{L}$, $\mathbf{G}_2 = \mathbf{L}^o$ and $\lambda = 1/2$ in the above equation yields:

$$\left(\overline{(\delta\mathbf{L} + \mathbf{L}^o)^{-1}}\right)^{-1} \geq \left(\overline{\delta\mathbf{L}^{-1}}\right)^{-1} + \left(\overline{\mathbf{L}^{o-1}}\right)^{-1}. \tag{49}$$

Therefore, the limit value, $\left(\overline{\mathbf{L}^{-1}}\right)^{-1}$, is the maximum value of $\mathbf{L}^*(x_3)$ and the optimal lower bound for the effective elastic properties of the plate is:

$$(\mathbf{A}^*, \mathbf{B}^*, \mathbf{D}^*)^- = \int_{-t/2}^{t/2} (1, x_3, x_3^2) \left(\overline{\mathbf{L}^{-1}}_{(i)(i)}\right)^{-1} (x_3)\, dx_3. \tag{50}$$

The optimal bounds obtained from Eq. (50) and Eq. (46) with the use of the Hashin-Shtrikman functional recover the bounds which were obtained by Kolpakov (1999) by using the Castigliano functional with a statically admissible in-plane stress field depending on x_3 and the Lagrange functional with a kinematically admissible out-of-plane displacement field depending on x_3.

These "first order" bounds, like the Voigt and Reuss bounds for an infinite medium, may be far from each other, especially if the plate is made of materials which exhibit a significant mechanical contrast. By focusing however on the polarizations in the phases, those bounds can be improved. We will do so in the next section by analyzing random heterogeneous plates.

4 Second order Bounds for Random Plates

A random distribution of the heterogeneities within the plate is now considered and information on second order correlation function of the elastic properties will be used. When the characteristic size of the structural material elements is large compared with that of the microstructure, the material can accurately be treated as locally homogeneous with spatially constant average properties. Many studies have been performed on such materials and used variational principles to derive lower and upper bounds for their overall properties (see e.g. Hashin and Shtrikman (1962a,b); Willis (1977, 1981)).

Moreover, for some materials the assumption of statistical homogeneity does not apply. Functionally graded materials (FGM) are examples of such materials. The continuous spatial variation of properties in those materials prevents the use of the methods developed for statistically uniform heterogeneous materials. For example, the work of Luciano and Willis (2004) applied the theory presented in Drugan and Willis (1996) to derive nonlocal constitutive equations for functionally graded materials. Several other micromechanical models have been proposed for the analysis of the overall thermomechanical properties of FGM (see e.g. Reiter and Dvorak (1997, 1998); Suresh and Mortensen (1998)).

This section aims at estimating bounds for the effective elastic properties of random plates. It is based on the Hashin-Shtrikman functional formulated in section 2. We assume that the constituent materials are randomly distributed and statistically homogeneous along directions which are parallel to the plane (x_1, x_2) of the plate and that the in-plane dimensions of the plate are large compared to its thickness.

4.1 n-Phase Random Plates

Let us now consider a composite with a random microstructure made of n phases whose geometrical distribution is characterized by α. Let ψ be the set of microstructures and $p(\alpha)$ the probability density of α in ψ. Thus, any property, f, of the material is a function of α and its ensemble average is defined as:

$$\mathbb{E}f(\alpha) = \int_{\psi} f(\alpha)\, p(\alpha)\, d\alpha. \tag{51}$$

Then, the probability $P_r(\mathbf{x})$ of finding the phase r at the location $\mathbf{x}$ is:

$$P_r(\mathbf{x}) = \mathbb{E}I_r(\mathbf{x}, \alpha) = \int_{\psi} I_r(\mathbf{x}, \alpha)\, p(\alpha)\, d\alpha, \tag{52}$$

where $I_r(\mathbf{x}, \alpha)$ is the indicator function of the region containing the phase r, $I_r(\mathbf{x}, \alpha) = 1$ when $\mathbf{x} \in Y_r$ and $I_r(\mathbf{x}, \alpha) = 0$ otherwise. Likewise, the two-point probability $P_{rs}(\mathbf{x}, \mathbf{x}')$ of finding simultaneously the phase r at the location $\mathbf{x}$ and the phase s at the location $\mathbf{x}'$ is:

$$P_{rs}(\mathbf{x}, \mathbf{x}') = \mathbb{E}(I_r(\mathbf{x}, \alpha) I_s(\mathbf{x}', \alpha)) = \int_{\psi} I_r(\mathbf{x}, \alpha)\, I_s(\mathbf{x}', \alpha)\, p(\alpha)\, d\alpha. \tag{53}$$

If phase r (where $r = 1, 2, \ldots, n$) is homogeneous and has a modulus $\mathbf{L}_r$, the elasticity tensor $\mathbf{L}(\mathbf{x})$ in sample α and its ensemble average are:

$$\mathbf{L}(\mathbf{x}, \alpha) = \sum_r L_r I_r(\mathbf{x}, \alpha), \quad \mathbb{E}\mathbf{L}(\mathbf{x}, \alpha) = \sum_r L_r P_r(\mathbf{x}). \tag{54}$$

Furthermore, we assume that the materials are statistically homogeneous along the (x_1, x_2)-directions. The characteristic properties are thus insensitive to translations along these directions:

$$P_r(\mathbf{x}) = P_r(x_3), \quad P_{rs}(\mathbf{x}, \mathbf{x}') = P_{rs}(\tilde{\mathbf{x}} - \tilde{\mathbf{x}}', x_3, x_3'). \tag{55}$$

Moreover, the polarization field in each phase is assumed to be not depending of x_1 and x_2, i.e., $\boldsymbol{\tau}_r(\mathbf{x}) = \boldsymbol{\tau}_r(x_3)$. In the following, the polarization field is assumed to be a linear combination of the indicator functions and can therefore be expressed as:

$$\boldsymbol{\tau}(\mathbf{x}, \alpha) = \sum_r \boldsymbol{\tau}_r(x_3) I_r(\mathbf{x}, \alpha). \tag{56}$$

As already mentioned, a common practice is to use the $\boldsymbol{\Gamma}$-operator for a periodic medium in the case of statistically homogeneous random media, as soon as the period is large enough compared to the correlation length (see e.g. Sab and Nedjar (2005)). This process will be used thereafter.

The previous definitions are introduced to enable the analysis of the ensemble average of the functional (30). Since W_o does not depend on $\boldsymbol{\tau}$, the total energy $W(\boldsymbol{\tau})$ and $W_1(\boldsymbol{\tau})$ have the same stationary point. Averaging the functional (32) now yields:

$$\begin{aligned}
\mathbb{E}W_1(\boldsymbol{\tau}) = \frac{1}{2} < 2 \sum_r \boldsymbol{\tau}_r(x_3) \boldsymbol{\epsilon}^o(x_3)\, P_r(x_3) - \sum_r \boldsymbol{\tau}_r(x_3) \delta \mathbf{L}_r^{-1} P_r(x_3) \boldsymbol{\tau}_r(x_3) \\
- \sum_r \sum_s \boldsymbol{\tau}_r(x_3) |Y|^{-1} \int_Y \boldsymbol{\Gamma}_p(\tilde{\mathbf{x}} - \tilde{\mathbf{x}}', x_3 - x_3') P_{rs}(\tilde{\mathbf{x}} - \tilde{\mathbf{x}}', x_3, x_3') \boldsymbol{\tau}_s(x_3')\, d\mathbf{x}' \\
- \sum_r \sum_s \boldsymbol{\tau}_r(x_3) |Y|^{-1} \int_Y \boldsymbol{\Gamma}_h(\tilde{\mathbf{x}} - \tilde{\mathbf{x}}', x_3, x_3') P_{rs}(\tilde{\mathbf{x}} - \tilde{\mathbf{x}}', x_3, x_3') \boldsymbol{\tau}_s(x_3')\, d\mathbf{x}' > .
\end{aligned} \tag{57}$$

where $\boldsymbol{\epsilon}^o(x_3)$ is the total strain field estimated in the reference medium. It is a deterministic function of x_3 .

4.2 Choice of the polarization tensor

We remind that the search for lower and upper bounds for the effective elastic properties of the plate can be performed by estimating the stationary value of the functional (57) . To this aim, one discretizes the plate along the x_3 and x_3' directions with N_3 points each. The polarization field in the phase is approximated by a piecewise function:

$$\boldsymbol{\tau}_r(x_3) = \sum_m \boldsymbol{\tau}_r^m \, I_m(x_3), \tag{58}$$

where I_m is the indicator function of the finite intervals whose union yields the part of the x_3-axis which is inside the plate. Therefore, the functional (57) can be rewritten as follows:

$$\mathbb{E}W_1 \simeq \frac{t}{2N_3} \sum_m \left[\sum_r 2\boldsymbol{\tau}_r^m \boldsymbol{\epsilon}_m^o \, P_r^m - \sum_r \boldsymbol{\tau}_r^m \delta \mathbf{L}_r^{-1} P_r^m \boldsymbol{\tau}_r^m \right.$$
$$\left. - \sum_{m'} \sum_r \sum_s \boldsymbol{\tau}_r^m \frac{1}{N_3|\omega|} \int_\omega \left(\boldsymbol{\Gamma}_p^{mm'}(\tilde{\mathbf{x}}') + \boldsymbol{\Gamma}_h^{mm'}(\tilde{\mathbf{x}}') \right) P_{rs}^{mm'}(\tilde{\mathbf{x}}') \boldsymbol{\tau}_s^{m'} \, d\tilde{\mathbf{x}}' \right], \tag{59}$$

where $\boldsymbol{\Gamma}_p^{mm'}(\tilde{\mathbf{x}}') = \boldsymbol{\Gamma}_p(\tilde{\mathbf{x}}', x_3(m) - x_3'(m'))$, $\boldsymbol{\Gamma}_h^{mm'}(\tilde{\mathbf{x}}') = \boldsymbol{\Gamma}_h(\tilde{\mathbf{x}}', x_3(m), x_3'(m'))$, $P_{rs}^{mm'}(\tilde{\mathbf{x}}') = P_{rs}(\tilde{\mathbf{x}}', x_3(m), x_3'(m'))$, $\boldsymbol{\epsilon}_m^o = \boldsymbol{\epsilon}^o(x_3(m))$, $P_r^m = P_r(x_3(m))$.

We notice that the integral expressions in (57) can be computed in the Fourier space with the wave vectors (k_1, k_2) using Parseval's theorem. For $m, m' = 1, \ldots, N_3$ points, Eq. (59) yields:

$$\mathbb{E}W_1 = \frac{t}{2N_3} \left(2\mathbf{T}^T \mathbf{F} - \mathbf{T}^T \mathbf{M}_l \, \mathbf{T} - \mathbf{T}^T \mathbf{M}_p \, \mathbf{T} - \mathbf{T}^T \mathbf{M}_h \, \mathbf{T} \right), \tag{60}$$

where $\mathbf{F}$, $\mathbf{M}_l$, $\mathbf{M}_p$ and $\mathbf{M}_h$ are linear and quadratic operators of the functional (59) and where the vector $\mathbf{T}$ is made of the discretized values of the polarization fields whose values are uniform in each discretized interval (see Eq. (58)):

$$\mathbf{T} = (\boldsymbol{\tau}_1^1, \ldots, \boldsymbol{\tau}_n^1, \ldots, \boldsymbol{\tau}_1^{N_3}, \ldots, \boldsymbol{\tau}_n^{N_3}) \quad \text{with} \quad \boldsymbol{\tau}_r^m = \boldsymbol{\tau}_r(x_3(m)), \tag{61}$$

where the polarization field in each phase is written under the form of a six-component vector (3D-problem): $(\tau_{11}, \tau_{22}, \tau_{33}, \tau_{23}, \tau_{13}, \tau_{12})^T$.

The vector $\mathbf{F}$ is computed from the 1-point probability function and from the strain field produced in the reference medium $\boldsymbol{\epsilon}^o(x_3)$. $\boldsymbol{\epsilon}^o(x_3)$ also is represented by a six component vector, $(\epsilon^o_{11}, \epsilon^o_{22}, \epsilon^o_{33}, 2\epsilon^o_{23}, 2\epsilon^o_{13}, 2\epsilon^o_{12})^T$. The symmetrical squared matrix $\mathbf{M}_l$ is determined from the 1-point probability function, the mechanical properties of the constituent materials and the mechanical properties of the reference medium. The squared matrices $\mathbf{M}_p$ and $\mathbf{M}_h$ are computed from the operators $\boldsymbol{\Gamma}_p$ and $\boldsymbol{\Gamma}_h$ and from the two-point probability function P_{rs}. Moreover, we notice that $\mathbf{M}_p$ and $\mathbf{M}_h$ are symmetrical matrices, since $\boldsymbol{\Gamma}_p$ and $\boldsymbol{\Gamma}_h$ are self-adjoint operators which verify: $\Gamma^p_{ijkl}(\mathbf{x}-\mathbf{x}') = \Gamma^p_{klij}(\mathbf{x}'-\mathbf{x})$ and $\Gamma^h_{ijkl}(\tilde{\mathbf{x}}-\tilde{\mathbf{x}}', x_3, x_3') = \Gamma^h_{klij}(\tilde{\mathbf{x}}'-\tilde{\mathbf{x}}, x_3', x_3)$.

The functional (60) is stationary when the following stationary condition is verified:

$$\mathbf{T}_s = (\mathbf{M}_l + \mathbf{M}_p + \mathbf{M}_h)^{-1}\,\mathbf{F}. \tag{62}$$

Hence, the stationary value of the average of the energy functional is obtained as:

$$\mathbb{E}W_1^s = \frac{t}{2N_3}\,\mathbf{T}_s^T\,\mathbf{F}. \tag{63}$$

The above value, used with Eq. (31), allows the computation of bounds for the effective elastic properties of the random plate. Those bounds vary with the choice of the reference medium and an appropriate choice of the elasticity tensor $\mathbf{L}^o$ enables the optimization of those bounds. The present theory was derived in the general case of random plates whose constituent materials are statistically homogeneous in the (x_1, x_2)-directions. To validate the steps described above, the simple case of an isotropic material is considered next. The estimated bounds for the homogenized elastic stiffnesses of a Love-Kirchhoff plate will enable to study the effects of the size of the heterogeneities on the values obtained for the bounds.

5 Application

5.1 Description of the microstructure

For performing an application of the results obtained previously, a Love-Kirchhoff plate made of two isotropic material phases is now considered and the different probability functions must be defined. The 1-point probability function $P_r(\mathbf{x})$ is the volume fraction c_r and the 2-point probability function is invariant by translation and rotation. Expressions derived analytically as well as numerically to estimate the two-point probability function exist for

numerous random material distributions (see e.g. Torquato (2001)). In the following, we consider a microstructure with a matrix containing a random distribution of non-overlapping spherical particles, for which the two-point probability function is given as follows (see e.g. Drugan and Willis (1996)):

$$P_{rs}(|\mathbf{x}-\mathbf{x}'|) = c_r c_s + c_r(\delta_{rs} - c_s)\, h(|\mathbf{x}-\mathbf{x}'|), \tag{64}$$

where c_r, c_s are the volume fractions of the phases r and s, respectively. This probability function is expressed in terms of the relative distance between two sampled points, namely $r = |\mathbf{x}-\mathbf{x}'|$. The function $h(r)$ can be expressed under an exponential form as (Drugan, 2003):

$$h(r) = e^{-\frac{r}{a}}, \tag{65}$$

where the coefficient a is a function of the radius R and of the volume fraction c_1 of the spherical inclusions (phase 1):

$$a^2 = R^2 \frac{5F_1 c_1 H_1 + 2G_1[H_1(2+c_1) - c_1(\tilde{c}_1/c_1)^{2/3}(9 - H_1 + \tilde{c}_1^2)]}{10G_1(1-c_1)H_1}, \tag{66}$$

where

$$\tilde{c}_1 = c_1 - \frac{1}{16}c_1^2,\ F_1 = \frac{3}{2}\frac{\tilde{c}_1^2(1 - 0.7117\tilde{c}_1 - 0.114\tilde{c}_1^2)}{(1-\tilde{c}_1)^4}. \tag{67}$$

$$G_1 = 12F_1\frac{(1-\tilde{c}_1)^2}{\tilde{c}_1(2+\tilde{c}_1)}, H_1 = 1 + 2\tilde{c}_1. \tag{68}$$

This expression is consistent with the numerical results obtained for example by Torquato and Stell (1985) who used the Percus and Yevick (1958) model of the statistical problem with random hard sphere distributions corrected by Verlet and Weis (1972) (see Drugan (2003) for details).

Figures 3 and 4 display the profiles of the two-point probability function along the in-plane direction in which the in-plane coordinate is normalized with respect to the diameter of the spherical inclusions. Moreover, since the inclusions cannot overlap, their concentration has an upper bound. This value is considered to be 0.64 (Torquato, 2001). One observes that the probability functions decrease and are then stationary. Figure 4 shows that the minimum in-plane correlation length is $10R$, above which a plateau appears.

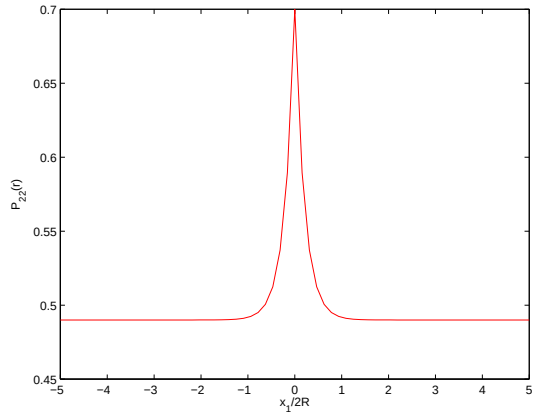

Figure 3: The two-point probability function, $P_{22}(r)$, $c_1 = 0.3$.

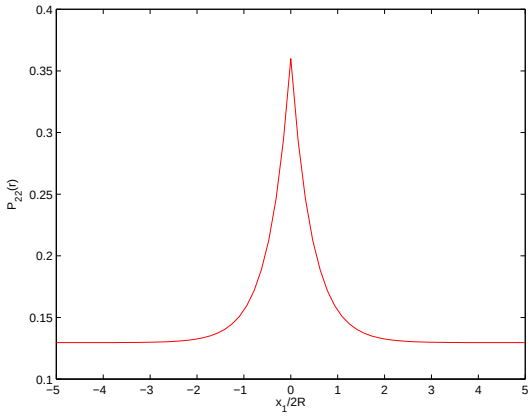

Figure 4: The two-point probability function, $P_{22}(r)$, $c_1 = 0.64$.

5.2 Numerical results

To apply numerically the theory described in the previous section, the computations are performed at the limit of a plane deformation problem in planes containing x_2-direction. A discretization of the space in the (x_1, x_3)-directions is necessary. The coordinates of the discretized points are defined as follows:

$$x_j = j\frac{l_j}{N_j}, \quad \text{with} \quad j = -\frac{N_j}{2}, \ldots, 0, \ldots, \frac{N_j}{2} - 1 \quad (j = 1, 3). \tag{69}$$

This discretization also is appropriate to use the Fast Fourier Transform (FFT), hence $N_j = 2^p$, $p \in \mathbb{N}^+$. The computation of the FFT corresponds to the wave-number order $n_j = [0, ..., \frac{N_j}{2} - 1, -\frac{N_j}{2}, ..., -1]$. The components of the wave vectors are then defined as follows: $k_j = 2\pi n_j / l_j$.

The homogenized elastic stiffnesses of the plate are obtained by an appropriate choice of the macroscopic strains $(\mathbf{E}, \boldsymbol{\chi})$ and by the computation of the extreme values of the energy functional W_o and $\mathbb{E}W_1^s$. This approximation will be compared with the stiffness properties of homogeneous plates whose elasticity tensors are computed from the classical Hashin-Shtrikman bounds in in infinite medium (UHS for the upper bound and LHS for the lower bound).

Figures 5 and 6 display comparisons of the bounds for the homogenized membrane and bending stiffnesses obtained from the theory developed in

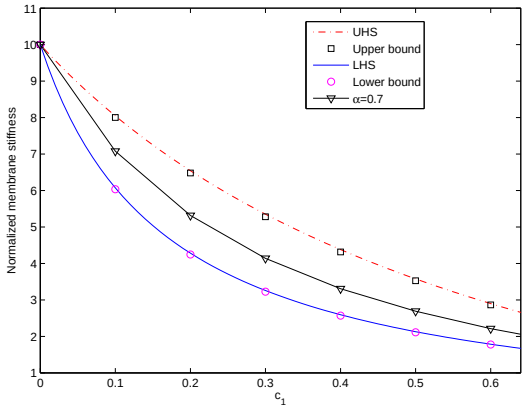

Figure 5: Comparison of the normalized bounds $A_{1111}/A_{1111}(E1)$ for the membrane stiffness in the case of small inclusions as a function of the concentration of material 1, $E_2/E_1 = 10$, $t/2R = 20$, $l_1/2R = 20$.

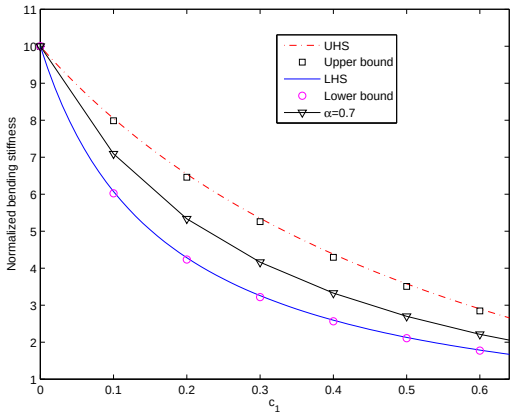

Figure 6: Comparison of the normalized bounds $D_{1111}/D_{1111}(E1)$ for the bending stiffness in the case of small inclusions as a function of the concentration of material 1, $E_2/E_1 = 10$, $t/2R = 20$, $l_1/2R = 20$.

this work with the stiffnesses derived from the classic solution of Hashin-Shtrikman in a case where the heterogeneities are small compared to the thickness of the plate.The values are expressed in terms of the concentration of phase 1 and normalized with the stiffnesses produced in a homogeneous medium with properties of phase 1. A discretization with $N_1 = N_3 = 2^7$ which ensures the convergence of the solution, was used for the computations. For comparison, values between the bounds are introduced, which are given by : $\mathbf{L}^o = \alpha\mathbf{L}_1 + (1-\alpha)\mathbf{L}_2$ with $\alpha = 0.7$.

It must be noticed that our optimized reference media for lower and upper bounds are identical to those computed for Hashin-Shtrikman bounds (Hashin and Shtrikman, 1962a,b), i.e., $\mathbf{L}^o = \mathbf{L}_1$ and $\mathbf{L}^o = \mathbf{L}_2$ ($\mathbf{L}_1 < \mathbf{L}_2$), respectively. Figures 5 and 6 allow to check that the stiffnesses computed from the classical bounds Hashin-Shtrikman bounds for infinite media are recovered by our computation, which is the waited result in the case where the plate thickness is large compared to the size of heterogeneities (here $t/2R = 20$)

After this first verification, a second study is performed to analyze the effect of the size of the period used in the computation of the Green tensor,

when it is compared to the radius of heterogeneities (related to the correlation length). Indeed, the Green's tensor for the plate which is known only for a periodic medium must be used for a length l_1 of the period which is large enough compared to the thickness of the plate and to the size of heterogeneities. The convergence of the stiffnesses of the plate for an increasing length of the period is now considered.

In a first step, the upper bound for the membrane stiffness is obtained for different values of l_1. Different period lengths were considered and it was found that it is not necessary to increase l_1 at values higher than $l_1 = 20R$. The stiffnesses were obtained for different values of the normalized in plane period defined by $l^* = l_1/2R$. They are reported in figure 7 where the upper bound for the membrane stiffness normalized with respect to its value for the computation at $l^* = 20$, $A = A_{1111}(l^*)/A_{1111}(l^* = 20)$ is given as a function of the concentration of material 1 for different values of l^*. It shows that the convergence is slower at higher concentration of inclusions.

To precise the level of convergence, a "relative error" r is defined from the normalized stiffnesses $M(l^*)$ (M being A_{111} or D_{1111} by the relationship:

$$\text{relative error}\, r(\%) = \frac{M(l^*) - M(l^* = 20)}{M(l^* = 20)} \times 100\%, \tag{70}$$

The results obtained for this relative error r are presented in table 1 for the case $c_1 = 0.64$ (for which the convergence is the slowest) showing that a relative error inferior to 0.5% is produced for $l^* = l_1/2R = 10$, which will be adopted in the following to study the effect of the size of the heterogeneities with respect to the ratio $t/2R$. These results confirm that *the Green tensor for the periodic plate can be used to study random plates as soon as the size of the period is large enough compared to the size of the heterogeneities.*

Now, it is posssible to reach the main objective of this work, which is to compute the Hashin-Shtrikman bounds for the plate and to compare these bounds with those obtained by using the elastic properties of plates computed from the Hashin-Shtrikman bounds of the elastic moduli related to an infinite medium. The bounds for the plate are compared for different values of the variable $t/2R$, which represents the ratio between the thickness of the plate and the size of heterogeneities. As shown previously, the stiffnesses of the plate computed from the Hashin-Shtrikman bounds in infinite media are recovered from the bounds computed for the plate when the thickness is large enough compared to the inclusion size. A comparison is therefore made by computing the normalized bound $B_p^* = \frac{B_p}{B_{HS}}$where B_p is the bound for A_{1111} or

Table 1: Relative error on the normalized stiffnesses of a random plate for different values of the period length l_1, $E_1/E_2 = 1/10$, $t/2R = 5$, $c_1 = 0.64$.

$l_1/2R$	r(A_{1111})(%)		r(D_{1111})(%)	
	lower bound	upper bound	lower bound	upper bound
5	1.82%	4.17%	2.51 %	5.26%
7.5	0.54%	1.32%	0.98 %	1.82%
10	0.12%	0.34%	0.38%	0.35%
15	-0.06%	-0.15%	-0.01%	-0.05%
20	0	0	0	0

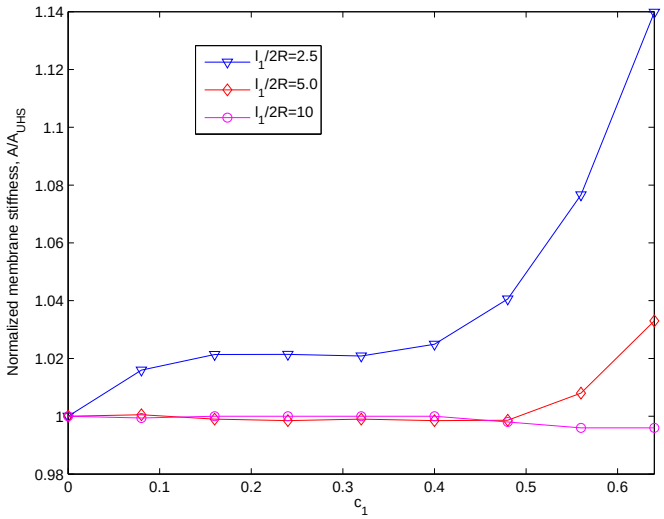

Figure 7: Normalized upper bound of the membrane stiffness (normalization with respect to the computation at $l^* = 20$), $E_2/E_1 = 10$, $t/2R = 5$.

D_{1111} computed from previous considerations and B_{HS} is the bound obtained by introducing into the plate properties the effective moduli produced by Hashin-Shtrikman bounds for infinite media.

These normalized bounds are computed in terms of $t/2R$ and reported in

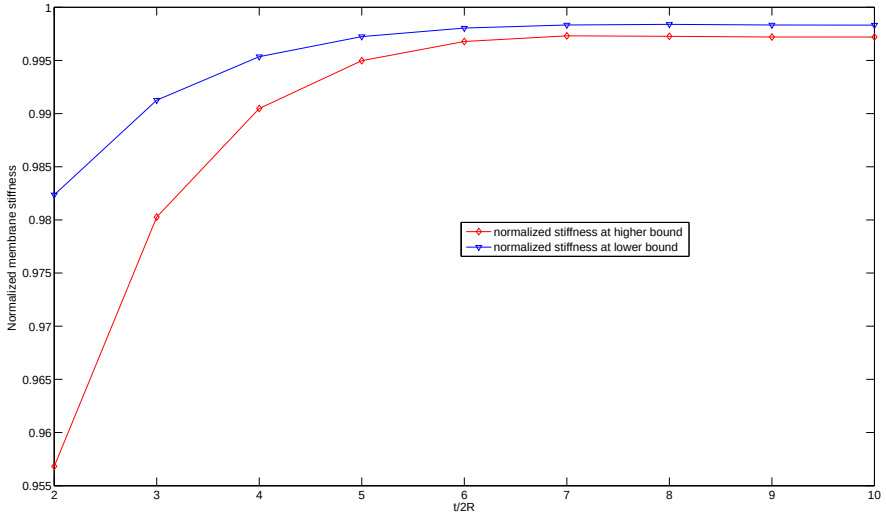

Figure 8: Normalized upper and lower bounds of the membrane stiffness as a function of the normalized thickness (normalization with respect to the stiffness obtained from H-S bounds for infinite media), $E_2/E_1 = 10$, $l_1/2R = 10$.

figures 8 and 9.

It can be seen that for large values of the thickness, the normalized stiffness becomes constant, and that the relative difference between B_p and B_{HS} becomes small (typically less than 1%) when the ratio $\frac{t}{2R}$ is large enough. The residual difference is of the order of the acceptation threshold chosen for the relative error induced by a limited period length. All results show that an estimation of the bounds for the plate from the HS bound for infinite media *overestimates* plate bounds, for both upper and lower bounds. This result confirms again that the bounds for the effective properties of the plate can be computed from the usual Hashin-Shtrikman bounds as soon as the thickness is large enough, compared to the size of the heterogeneities. The difference between both bounds increases when the ratio $\frac{t}{2R}$ decreases below a threshold around 6. The ratio between bounds reaches smaller values for the upper bound and for the bending stiffness, but the difference between plate bounds and plate properties computed from Hashin-Shtrikman bounds for infinite media still remains inferior to 10% in all cases. This result is compatible with results obtained by other authors in relation with the minimum

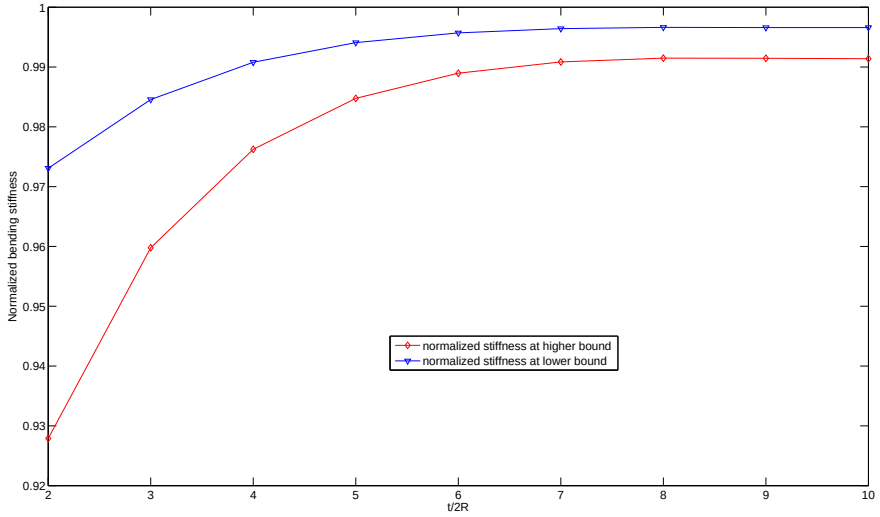

Figure 9: Normalized upper and lower bounds of the curvature stiffness as a function of the normalized stiffness (normalization with respect to the stiffness obtained from H-S bounds for infinite media), $E_2/E_1 = 10$, $l_1/2R = 10$.

size of the "Representative Volume Element" which is often found around five to six times the heterogeneity size.

6 Conclusions

This paper has presented the results obtained from the Hashin-Shtrikman variational principle for heterogeneous plates when using within the variational principle a $\mathbf{\Gamma}$-operator with stress-free boundary conditions. Two applications were considered. First, a polarization which does not depend of the position within a plan parallel to the plate is introduced within the variational principle. The bounds which are thus obtained coincide with "first order" refined estimates of the Voigt and Reuss bounds proposed by Kolpakov (1999) for heterogeneous plates. The optimized polarization fields which are used for reaching the bounds are related to null and infinite elastic moduli of the reference medium introduced within the variational principle.

In the second application, the Hashin-Shtrikman variational formulation is used for random heterogeneous plates. The assumption of a statistically

uniform distribution of the materials along the in-plane directions of the plate yielded a simplified expression of the functional in terms of the in-plane invariant polarizations.

A simple example with isotropic materials was considered and allowed to predict the effect of the size of the heterogeneities on "second order" bounds of the effective properties of plates. The statistical distribution of the heterogeneities is entirely defined by its two points probability function as introduced by Torquato (2001) and does not require Monte Carlo computations or ensemble averagings. The "second-order" bounds for the homogenized elastic properties of the plate were compared with those obtained by computing plate properties from classical Hashin-Shtrikman (HS) bounds for elastic effective properties (Hashin and Shtrikman, 1962a,b, 1965). A natural estimation of bounds for elastic (membrane and stiffness) plate stiffnesses is indeed to compute the HS bounds for elastic properties in an infinite medium and to introduce these bounding elastic properties into plate stiffnesses . Our results show that such a procedure leads to correct results for a ratio "thickness"/"heterogeneity size" which is greater than a threshold around 6. For such a ratio being lower, the estimation of bounds by such a procedure overestimates the bounds for plate properties.

APPENDIX

A Solution of the auxiliary problem and calculation of the related operators

The Fourier method is used to solve the problem (16) for which any periodic function $g(\mathbf{x})$ can be expanded into the Fourier series,

$$g(\mathbf{x}) = \sum_{\mathbf{k}} \hat{g}(\mathbf{k})\, e^{i\mathbf{k}.\mathbf{x}}, \quad \hat{g}(\mathbf{k}) = \frac{1}{|Y|}\int_Y g(\mathbf{x})\, e^{-i\mathbf{k}.\mathbf{x}} d\mathbf{x}, \tag{71}$$

where $\mathbf{k} = (k_1, k_2, k_3)$ or $\tilde{\mathbf{k}} = (k_1, k_2)$ used in the sequel denote the discrete wave vectors arranged along a discrete lattice having a period $2\pi/l_i$ ($l_3 = t$) in the direction x_i.

To solve the boundary value problem (16), the solution fields are split into two components: a standard periodic component obtained from (18) and a complementary component derived from (20) to recover boundary conditions. For the periodic solution field, the resolution of (18) can be performed using the Fourier transforms (Suquet, 1990; Moulinec and Suquet, 1994). In fact, after transformations into the Fourier space of the equilibrium equation, the constitutive equation, the compatibility relation and elimination of $\hat{\sigma}^p_{ij}(\mathbf{k})$ between the equations, the periodic strains of (18) can then be obtained in the Fourier space by means of the periodic $\mathbf{\Gamma}_p$-operator associated to the homogeneous reference medium with stiffness $\mathbf{L}^o$,

$$\hat{\mathbf{e}}^p(\mathbf{k}) = -\hat{\mathbf{\Gamma}}_p(\mathbf{k}) : \hat{\boldsymbol{\tau}}(\mathbf{k}) \quad \forall \mathbf{k} \neq 0, \quad \hat{\mathbf{e}}^p(0) = 0. \tag{72}$$

In real space, the periodic strains $\mathbf{e}^p(\mathbf{x})$ are given by (19) under a convolution product formulated according to the definition (71). The Fourier components of the $\mathbf{\Gamma}_p$-operator are explicitly given in Mura (1991) for different types of anisotropy for the homogeneous medium. For an isotropic material with Lamé coefficients (λ, μ), it takes the form:

$$\hat{\Gamma}^p_{ijkl} = \frac{1}{4\mu|\mathbf{k}|^2}(\delta_{ik}k_jk_l + \delta_{jk}k_ik_l + \delta_{il}k_jk_k + \delta_{jl}k_ik_k) - \frac{\lambda+\mu}{\mu(\lambda+2\mu)}\frac{k_ik_jk_kk_l}{|\mathbf{k}|^4}. \tag{73}$$

It should be noted that $\mathbf{\Gamma}_p$ is a self-adjoint operator and due to parity of the tensor $\hat{\mathbf{\Gamma}}_p(\mathbf{k})$, the following property is verified: $\mathbf{\Gamma}_p(\mathbf{x}-\mathbf{x}') = \mathbf{\Gamma}_p(\mathbf{x}'-\mathbf{x})$.

Furthermore, the resolution of the complementary problem (20) is performed using the Fourier transformations along the periodic directions (x_1, x_2) such that the solution field can be defined as follows:

$$\left(\mathbf{u}^h(\mathbf{x}), \mathbf{e}^h(\mathbf{x}), \boldsymbol{\sigma}^h(\mathbf{x})\right) = \sum_{\tilde{\mathbf{k}}} \left(\tilde{\mathbf{u}}^h(\tilde{\mathbf{k}}, x_3), \tilde{\mathbf{e}}^h(\tilde{\mathbf{k}}, x_3), \tilde{\boldsymbol{\sigma}}^h(\tilde{\mathbf{k}}, x_3)\right) \, e^{ik_\alpha x_\alpha}. \quad (74)$$

Using the Fourier transforms along (x_1, x_2), the strain field is related to the displacement field by: $\tilde{\mathbf{e}}^h\left(\tilde{\mathbf{k}}, x_3\right) = \tilde{\mathbf{u}}^h\left(\tilde{\mathbf{k}}, x_3\right) \otimes^s \boldsymbol{\nabla}'$ where the operator $\boldsymbol{\nabla}'$ is defined by $\boldsymbol{\nabla}' = \begin{bmatrix} ik_1 & ik_2 & \partial_3 \end{bmatrix}^T$. The operator ∂ indicates the partial differentiation with respect to the coordinate subscript that follows. Supposing that the material is isotropic, the equilibrium equation $\boldsymbol{\sigma}^h\left(\mathbf{x}\right).\boldsymbol{\nabla} = 0$ becomes $\tilde{\boldsymbol{\sigma}}^h\left(\tilde{\mathbf{k}}, x_3\right).\boldsymbol{\nabla}' = 0$ which leads to

$$\left[(\lambda + \mu)\boldsymbol{\nabla}' \otimes^s \boldsymbol{\nabla}' + \mu(\boldsymbol{\nabla}'.\boldsymbol{\nabla}')\,\mathbf{1}\right].\tilde{\mathbf{u}}^h\left(\tilde{\mathbf{k}}, x_3\right) = 0, \quad (75)$$

where,

$$\boldsymbol{\nabla}' \otimes^s \boldsymbol{\nabla}' = \begin{bmatrix} -k_1^2 & -k_1k_2 & ik_1\partial_3 \\ -k_1k_2 & -k_2^2 & ik_2\partial_3 \\ ik_1\partial_3 & ik_2\partial_3 & \partial_{33}^2 \end{bmatrix}, \quad \boldsymbol{\nabla}'.\boldsymbol{\nabla}' = \partial_{33}^2 - (k_1^2 + k_2^2). \quad (76)$$

The solution of equation (75) is :

$$\tilde{\mathbf{u}}^h(\tilde{\mathbf{k}}, x_3) = \left(\mathbf{a}^+ + x_3\mathbf{b}^+\right) e^{sx_3} + \left(\mathbf{a}^- + x_3\mathbf{b}^-\right) e^{-sx_3}, \quad (77)$$

where:

$$\mathbf{a}^\pm = \begin{Bmatrix} a_1^\pm \\ a_2^\pm \\ \pm\frac{1}{is}(a_1^\pm k_1 + a_2^\pm k_2 - i\frac{\lambda+3\mu}{\lambda+\mu}b_3^\pm) \end{Bmatrix}, \; \mathbf{b}^\pm = \begin{Bmatrix} \pm\frac{ik_1}{s}b_3^\pm \\ \pm\frac{ik_2}{s}b_3^\pm \\ b_3^\pm \end{Bmatrix}, \; s = \sqrt{k_1^2 + k_2^2}. \quad (78)$$

The six complex coefficients $(a_1^\pm, a_2^\pm, b_3^\pm)$ are obtained from the six boundary conditions defined in (20) which are rewritten as follows:

$$\tilde{\sigma}_{j3}^h(\tilde{\mathbf{k}}, \pm\frac{t}{2}) = -\sum_{k_3} \hat{\sigma}_{j3}^p(\mathbf{k}) e^{\pm ik_3\frac{t}{2}}. \quad (79)$$

More precisely, the 3 boundary conditions at the top face ($x_3 = t/2$) and the 3 boundary conditions at the bottom face ($x_3 = -t/2$) of the unit cell enable to construct a system of 6 equations for determining 6 coefficients of the vector $\boldsymbol{\xi} = (a_1^+, a_1^-, a_2^+, a_2^-, b_3^+, b_3^-)$,

$$\mathbf{K}\boldsymbol{\xi} = \mathbf{q}, \tag{80}$$

where

$$\mathbf{K} = \begin{bmatrix}
\frac{\mu}{s}(s^2+k_1^2)e^{s\frac{t}{2}} & -\frac{\mu}{s}(s^2+k_1^2)e^{-s\frac{t}{2}} & \frac{\mu}{s}k_1k_2e^{s\frac{t}{2}} & -\frac{\mu}{s}k_1k_2e^{-s\frac{t}{2}} & 2\frac{\mu}{s}ik_1\gamma^-e^{s\frac{t}{2}} & 2\frac{\mu}{s}ik_1\gamma^+e^{-s\frac{t}{2}} \\
\frac{\mu}{s}(s^2+k_1^2)e^{-s\frac{t}{2}} & -\frac{\mu}{s}(s^2+k_1^2)e^{s\frac{t}{2}} & \frac{\mu}{s}k_1k_2e^{-s\frac{t}{2}} & -\frac{\mu}{s}k_1k_2e^{s\frac{t}{2}} & -2\frac{\mu}{s}ik_1\gamma^+e^{-s\frac{t}{2}} & -2\frac{\mu}{s}ik_1\gamma^-e^{s\frac{t}{2}} \\
\frac{\mu}{s}k_1k_2e^{s\frac{t}{2}} & -\frac{\mu}{s}k_1k_2e^{-s\frac{t}{2}} & \frac{\mu}{s}(s^2+k_2^2)e^{s\frac{t}{2}} & -\frac{\mu}{s}(s^2+k_2^2)e^{-s\frac{t}{2}} & 2\frac{\mu}{s}ik_2\gamma^-e^{s\frac{t}{2}} & 2\frac{\mu}{s}ik_2\gamma^+e^{-s\frac{t}{2}} \\
\frac{\mu}{s}k_1k_2e^{-s\frac{t}{2}} & -\frac{\mu}{s}k_1k_2e^{s\frac{t}{2}} & \frac{\mu}{s}(s^2+k_2^2)e^{-s\frac{t}{2}} & -\frac{\mu}{s}(s^2+k_2^2)e^{s\frac{t}{2}} & -2\frac{\mu}{s}ik_2\gamma^+e^{-s\frac{t}{2}} & -2\frac{\mu}{s}ik_2\gamma^-e^{s\frac{t}{2}} \\
-2\mu ik_1e^{s\frac{t}{2}} & -2\mu ik_1e^{-s\frac{t}{2}} & -2\mu ik_2e^{s\frac{t}{2}} & -2\mu ik_2e^{-s\frac{t}{2}} & 2\mu\eta^-e^{s\frac{t}{2}} & -2\mu\eta^+e^{-s\frac{t}{2}} \\
-2\mu ik_1e^{-s\frac{t}{2}} & -2\mu ik_1e^{s\frac{t}{2}} & -2\mu ik_2e^{-s\frac{t}{2}} & -2\mu ik_2e^{s\frac{t}{2}} & -2\mu\eta^+e^{-s\frac{t}{2}} & 2\mu\eta^-e^{s\frac{t}{2}}
\end{bmatrix}, \tag{81}$$

with $\gamma^\pm = s\frac{t}{2} \pm \frac{\mu}{\lambda+\mu}$, $\eta^\pm = s\frac{t}{2} \pm \frac{\lambda+2\mu}{\lambda+\mu}$, and the components of the vector $\mathbf{q} = (q_1^+, q_1^-, q_2^+, q_2^-, q_3^+, q_3^-)$ being defined in (84). The closed-form solution of (80) can be found in Nguyen et al. (2008).

Moreover, the strain $\tilde{\mathbf{e}}^h(\tilde{\mathbf{k}}, x_3)$ for $|\tilde{\mathbf{k}}| \neq 0$ ($s \neq 0$) is obtained from the compatibility equation. It can be expressed by usiing a matrix $\mathbf{P}(\tilde{\mathbf{k}}, x_3)$ and the vector $\boldsymbol{\xi}(\tilde{\mathbf{k}})$ as of form:

$$\tilde{\mathbf{e}}^h(\tilde{\mathbf{k}}, x_3) = \mathbf{P}(\tilde{\mathbf{k}}, x_3)\,\xi(\tilde{\mathbf{k}}) = \mathbf{P}(\tilde{\mathbf{k}}, x_3)\,\mathbf{K}^{-1}(\tilde{\mathbf{k}})\,\mathbf{q}(\tilde{\mathbf{k}}), \tag{82}$$

where

$$\mathbf{P} = \begin{bmatrix}
ik_1e^{sx_3} & ik_1e^{-sx_3} & 0 & 0 & -\frac{k_1^2}{s}x_3e^{sx_3} & \frac{k_1^2}{s}x_3e^{-sx_3} \\
0 & 0 & ik_2e^{sx_3} & ik_2e^{-sx_3} & -\frac{k_2^2}{s}x_3e^{sx_3} & \frac{k_2^2}{s}x_3e^{-sx_3} \\
-ik_1e^{sx_3} & -ik_1e^{-sx_3} & -ik_2e^{sx_3} & -ik_2e^{-sx_3} & (x_3s - \frac{2\mu}{\lambda+\mu})e^{sx_3} & -(x_3s + \frac{2\mu}{\lambda+\mu})e^{-sx_3} \\
\frac{k_1k_2}{2s}e^{sx_3} & -\frac{k_1k_2}{2s}e^{-sx_3} & \frac{s^2+k_2^2}{2s}e^{sx_3} & -\frac{s^2+k_2^2}{2s}e^{-sx_3} & \frac{ik_2}{s}(x_3s - \frac{\mu}{\lambda+\mu})e^{sx_3} & \frac{ik_2}{s}(x_3s + \frac{\mu}{\lambda+\mu})e^{-sx_3} \\
\frac{s^2+k_1^2}{2s}e^{sx_3} & -\frac{s^2+k_1^2}{2s}e^{-sx_3} & \frac{k_1k_2}{2s}e^{sx_3} & -\frac{k_1k_2}{2s}e^{-sx_3} & \frac{ik_1}{s}(x_3s - \frac{\mu}{\lambda+\mu})e^{sx_3} & \frac{ik_1}{s}(x_3s + \frac{\mu}{\lambda+\mu})e^{-sx_3} \\
\frac{ik_2}{2}e^{sx_3} & \frac{ik_2}{2}e^{-sx_3} & \frac{ik_1}{2}e^{sx_3} & \frac{ik_1}{2}e^{-sx_3} & -\frac{k_1k_2}{s}x_3e^{sx_3} & \frac{k_1k_2}{s}x_3e^{-sx_3}
\end{bmatrix}, \tag{83}$$

and the components of the vector $\mathbf{q}(\tilde{\mathbf{k}}) = (q_1^+, q_1^-, q_2^+, q_2^-, q_3^+, q_3^-)$ are derived from the boundary conditions (79). They are expressed in terms of the periodic stresses, $\hat{\boldsymbol{\sigma}}^p(\mathbf{k})$, in the Fourier space as:

$$q_j^{\pm} = -\sum_{k_3} e^{\pm ik_3 \frac{t}{2}}\, \hat{\sigma}_{j3}^p(\mathbf{k}) = -\sum_{k_3} e^{\pm ik_3 \frac{t}{2}}\, \hat{\delta}_{j3mn}(\mathbf{k})\, \hat{\tau}_{mn}(\mathbf{k}), \tag{84}$$

where $\hat{\boldsymbol{\delta}}(\mathbf{k}) = \mathbf{I} - \mathbf{L}^o\, \hat{\boldsymbol{\Gamma}}_p(\mathbf{k})$.

It may be noticed that $\hat{\boldsymbol{\delta}}(\mathbf{k})$ is calculated with $\mathbf{k} \neq 0$ and it is reduced to the unity matrix $\mathbf{I}$ for $\mathbf{k} = 0$. Therefore, the relation (84) allows to construct a matrix $\mathbf{S}(\mathbf{k})$ constituted from the product $e^{\pm ik_3 \frac{t}{2}}\, \hat{\delta}_{j3mn}(\mathbf{k})$ according to the corresponding vector $\mathbf{q}(\tilde{\mathbf{k}})$ leading to:

$$\mathbf{q}(\tilde{\mathbf{k}}) = -\sum_{k_3} \mathbf{S}(\mathbf{k})\, \hat{\boldsymbol{\tau}}(\mathbf{k}). \tag{85}$$

Substituting the above expression into (82) and taking into account the Fourier transformation in x_3' of the polarization tensor leads to

$$\tilde{\mathbf{e}}^h(\tilde{\mathbf{k}}, x_3) = -\frac{1}{t} \int_{-t/2}^{t/2} \tilde{\boldsymbol{\Gamma}}_h(\tilde{\mathbf{k}}, x_3, x_3')\, \tilde{\boldsymbol{\tau}}(\tilde{\mathbf{k}}, x_3')\, dx_3', \tag{86}$$

where $\tilde{\boldsymbol{\Gamma}}_h(\tilde{\mathbf{k}}, x_3, x_3')$ at the given points (x_3, x_3') is defined by

$$\tilde{\boldsymbol{\Gamma}}_h(\tilde{\mathbf{k}}, x_3, x_3') = \mathbf{P}(\tilde{\mathbf{k}}, x_3)\, \mathbf{K}^{-1}(\tilde{\mathbf{k}}) \sum_{k_3} \mathbf{S}(\mathbf{k})\, e^{-ik_3 x_3'}. \tag{87}$$

It should be noted that this expression is calculated with $\tilde{\mathbf{k}} \neq 0$, its value at $\tilde{\mathbf{k}} = 0$ is also considered from the corresponding strains. Moreover, taking into account the definition (71), the complementary strains can be written in the real space as (21).

For $|\tilde{\mathbf{k}}| = 0$, the membrane strains $\tilde{e}_{\alpha\beta}^h$ are null due to the periodicity on ∂Y_l of the displacement field, i.e. $\tilde{e}_{\alpha\beta}^h(\tilde{\mathbf{k}} = 0, x_3) = 0$. The calculation of $\tilde{e}_{j3}^h(\tilde{\mathbf{k}} = 0, x_3)$ is also performed by using the boundary condition (79) and the differential equation system (75). This gives the expressions of the out-of-plane strain field as follows,

$$\tilde{e}_{33}^h(\tilde{\mathbf{k}} = 0, x_3) = -\frac{1}{\lambda + 2\mu} \sum_{k_3} \hat{\sigma}_{33}^p(\tilde{\mathbf{k}} = 0, k_3)\, e^{ik_3 \frac{t}{2}}, \tag{88}$$

$$\tilde{e}^h_{\alpha 3}(\tilde{\mathbf{k}}=0,x_3) = -\frac{1}{2\mu}\sum_{k_3}\hat{\sigma}^p_{\alpha 3}(\tilde{\mathbf{k}}=0,k_3)\,e^{ik_3\frac{t}{2}}. \tag{89}$$

For estimating the values of $\hat{\sigma}^p_{j3}$ at $\tilde{\mathbf{k}}=0$, it is noted that the out-of-plane stresses, $\hat{\sigma}^p_{j3}$, are null for the case of $\tilde{\mathbf{k}}=0$ and $k_3\neq 0$. As a consequence, the calculation of the out-of-plane complementary strains in (88) and (89) is reduced to the case of $\mathbf{k}=0$ where $\hat{\sigma}^p_{j3}(\mathbf{k}=0)=\hat{\tau}_{j3}(\mathbf{k}=0)$:

$$\tilde{e}^h_{33}(\tilde{\mathbf{k}}=0,x_3) = -\frac{\hat{\tau}_{33}(\mathbf{k}=0)}{\lambda+2\mu}, \quad \tilde{e}^h_{\alpha 3}(\tilde{\mathbf{k}}=0,x_3) = -\frac{\hat{\tau}_{\alpha 3}(\mathbf{k}=0)}{2\mu}. \tag{90}$$

It allows to determine the non-null components of the $\tilde{\mathbf{\Gamma}}_h$ at $\tilde{\mathbf{k}}=0$ as follows: $\tilde{\Gamma}^h_{3333}(\tilde{\mathbf{k}}=0,x_3)=1/(\lambda+2\mu)$ and $\tilde{\Gamma}^h_{\alpha 3\alpha 3}(\tilde{\mathbf{k}}=0,x_3)=1/2\mu$.

References

Bonnet, G., 2007. Effective properties of elastic periodic composite media with fibers. J. Mech. Phys. Solids 55(5), 881–899.

Bourgeois, S., Débordes, O., Patou, P., 1998. Homogénéisation et plasticité des plaques minces. Rev. Eur. Elem. Finis 7, 39–54.

Caillerie, D., 1984. Thin elastic and periodic plates. Math. Meth. Appl. Sci. 6, 159–191.

Cecchi, A., Sab, K., 2002a. A multi-parameter homogenization study for modelling elastic masonry. Euro. J. Mech. A/Solids 21, 249–268.

Cecchi, A., Sab, K., 2002b. Out of plane model for heterogenous periodic materials: the case of masonry. Euro. J. Mech. A/Solids 21, 715–746.

Cecchi, A., Sab, K., 2004. A comparison between a 3d discrete model and two homogenized plate models for periodic elastic brickword. Int. J. Solids Struct. 41, 2259–2276.

Dallot, J., Sab, K., 2008a. Limit analysis of multi-layered plates. Part I: The homogenized Love-Kirchhoff model. J. Mech. Phys. Solids 56, 561–580.

Dallot, J., Sab, K., 2008b. Limit analysis of multi-layered plates. Part II: Shear effects. J. Mech. Phys. Solids 56, 581–612.

Drugan, W. J., 2003. Two exact micromechanics-based nonlocal constitutive equations for random linear elastic composite materials. J. Mech. Phys. Solids 51, 1745–1772.

Drugan, W. J., Willis, J. R., 1996. A micromechanics-based nonlocal constitutive equation and estimates of representative volume element size for elastic composites. J. Mech. Phys. Solids 44, 497–524.

Duvaut, G., Metellus, A. M., 1976. Homogénéisation d'une plaque mince en flexion des structures périodique et symétrique. C.R. Acad. Sci. Sér. A. 283, 947–950.

Hashin, Z., Shtrikman, S., 1962a. On some variational principles in anisotropic and nonhomogeneous elasticity. J. Mech. Phys. Solids 10, 335–342.

Hashin, Z., Shtrikman, S., 1962b. A variational approach to the theory of elastic behavior of polycrystals. J. Mech. Phys. Solids 10, 343–352.

Hashin, Z., Shtrikman, S., 1965. On elastic behavior of fibre reinforced materials of arbitrary transverse phase geometry. J. Mech. Phys. Solids 13, 119–134.

Hashin, Z., Shtrikman, S., 1967. Variational priciples of elasticity in terms of the polarization. Int. J. Eng. Sci. 5, 213–223.

Hill, R., 1952. The elastic behavior of a crystalline aggregate. Proce. Phys. Soc. 65, 349–354.

Kohn, R. V., Vogelius, M., 1984. A new model for thin plates with rapidly varying thickness. Int. J. Solids Struct. 20, 333–350.

Kolpakov, A. G., 1998. Variational principles for stiffnesses of a non-homogeneous beams. J. Meth. Phys. Solids 46, 1039–1053,.

Kolpakov, A. G., 1999. Variational principles for stiffnesses of a non-homogeneous plate. J. Meth. Phys. Solids 47, 2075–2092,.

Kolpakov, A. G., Sheremet, I. G., 1999. The stiffnesses of non-homogeneous plates. J. Appl. Maths. Mechs. 63, 633–640,.

Lewiński, T., Telega, J., 2000. Plates, Laminates and Shells: Asymptotic Analysis and Homogenization. World Scientific Publishing.

Luciano, R., Willis, J. R., 2004. Non-local constitutive equations for functionally graded materials. Mech. Mater. 36, 1195–1206.

Moulinec, H., Suquet, P., 1994. A fast numerical method for computing the linear and nonlinear properties of composites. C.R. Acad. Sci. 318, 1417–1423.

Moulinec, H., Suquet, P., 1998. A numerical method for computing the overall response of nonlinear composites with complex microstructure. Compu. Meth. Appl. Mech. Eng. 157, 69–94.

Mura, T., 1991. Micromechanics of deflects in solids. Kluwer Academic Publisers.

Nguyen, T. K., Sab, K., Bonnet, G., 2008. Green's operator for a periodic medium with traction-free boundary conditions and computation of the effective properties of thin plates. Int. J. Solids Struct. 45(25-26), 6518–6534.

Percus, J. K., Yevick, G. J., 1958. Analysis of classical statistical mechanics by means of collective coordinates. Phys. Rev. 110, 1–13.

Reiter, T., Dvorak, G. J., 1997. Micromechanical models for graded composite materials. J. Mech. Phys. Solids 45, 1281–1302.

Reiter, T., Dvorak, G. J., 1998. Micromechanical models for graded composite materials: II. Thermomechanical loading. J. Mech. Phys. Solids 46, 1655–1673.

Sab, K., 2003. Yield design of thin periodic plates by a homogenization technique and an application to masonry wall. C. R. Mécanique 331, 641–646.

Sab, K., Nedjar, B., 2005. Periodization of random media and representative volume element size for linear composites. C. R. Mécanique 333, 187–195.

Suquet, P., 1990. Une méthode simplifiée pour le calcul des propriétés élastiques de matériaux hétérogènes à structure périodique. C.R. Acad. Sci. 311, 769–774.

Suresh, S., Mortensen, A., 1998. Fundamentals of functionally graded materials: Processing and Thermomechanical Behaviour of Graded Metals and Metal-Ceramic Composites. Press, Cambridge.

Torquato, S., 2001. Random Heterogeneous Materials - Microstructure and Macroscopic properties. Springer, New York.

Torquato, S., Stell, G., 1985. Microstructure of two-phase random media. V. the n-point matrix probability functions for impenetrable spheres. J. Chem. Phys. 82, 980–987.

Verlet, L., Weis, J. J., 1972. Equilibrium theory of simple liquids. Phys. Rev. A 5, 939–952.

Willis, J. R., 1977. Bounds and self-consistent estimates for the overall properties of anisotropic composites. J. Mech. Phys. Solids 25, 185–202.

Willis, J. R., 1981. Variational and related methods for the overall properties of composites. Adva. Appl. Mech. 21, 1–78.